Developmental Biology 451 (2019) 53–67

Contents lists available at ScienceDirect

Developmental Biology

journal homepage: www.elsevier.com/locate/developmentalbiology

Review article

Mechanisms that regulate morphogenesis of a highly branched neuron in *C. elegans*

Lakshmi Sundararajan, Jamie Stern, David M. Miller III *

Department of Cell and Developmental Biology, Vanderbilt University, Nashville, TN 37240, USA

A B S T R A C T

The shape of an individual neuron is linked to its function with axons sending signals to other cells and dendrites receiving them. Although much is known of the mechanisms for axonal outgrowth, the striking complexity of dendritic architecture has hindered efforts to uncover pathways that direct dendritic branching. Here we review the results of an experimental strategy that exploits the power of genetic analysis and live cell imaging of the PVD sensory neuron in *C. elegans* to reveal key molecular drivers of dendrite morphogenesis.

1. Introduction

To function as biological communication devices, neurons adopt polarized morphologies by extending dendrites to detect signals and axons to release them. These functional differences are correlated with structural features unique to either dendrites or axons. For example, a neuron may give rise to multiple dendrites but typically only one axon. In addition, dendrite architecture can be highly complex. This characteristic is particularly striking for cerebellar Purkinje neurons, for instance, which may display a dendritic arbor of hundreds of branches. The distinctive pattern of dendrite branching unique to each type of neuron points to a key role for dendrite architecture in neuronal function. Despite this clear link between dendrite morphology and function, much more is known about the mechanisms that direct axon outgrowth than the pathways that shape dendrite branching. This disparity is likely a consequence of the striking diversity and complexity of dendritic arbors which hinders direct analysis of branching mechanisms. Recent work in *C. elegans*, however, has substantially advanced our understanding of dendrite morphogenesis by exploiting the accessibility of the PVD sensory neuron to live cell imaging and genetic analysis.

2. PVD neurons adopt a highly branched dendritic arbor to function as a polymodal nociceptors

The *C. elegans* nervous system is highly compact. Most *C. elegans* neurons display unbranched neurites that are bundled in the nerve ring in the head or in fascicles oriented along the body axis. A subset of *C. elegans* neurons extend branches but these are typically limited in number. Specific motor neurons, for example, project single circumferential processes or commissures from ventral to dorsal nerve cords (White et al., 1986). A notable exception is the PVD somatosensory neuron which is highly branched and located in a posterior-lateral position. *C. elegans* contains two PVD neurons, one each on the right (PVDR) and left (PVDL) sides of the animal. In the adult, PVD neurons display a striking, orthogonal array of dendritic branches that envelop the body terminating near the posterior bulb of the pharynx in the neck region (Albeg et al., 2011; Oren-Suissa et al., 2010; Smith et al., 2010). The head is covered by a similar highly branched dendritic arbor arising from the FLPR and FLPL neurons (Albeg et al., 2011; Smith et al., 2010). Together, PVD and FLP swathe the entire animal with a net-like array of sensory processes that respond to harsh mechanical force (Chatzigeorgiou et al., 2010; Way and Chalfie, 1989) (Fig. 1A). PVD also detects additional noxious stimuli (extreme temperature, hyperosmolarity) and may function as a proprioceptor to regulate body posture (Albeg et al., 2011; Chatzigeorgiou et al., 2010; Li et al., 2011; Mohammadi et al., 2013; Smith et al., 2013). Here we review progress toward understanding the molecular pathways that direct PVD branching morphogenesis.

As originally reconstructed by serial section electron microscopy (EM), PVD featured a simple morphology with the cell soma giving rise to a bilateral pair of 1^0, unbranched neurites that extend in opposite directions along the lateral nerve cord and a single axon that projects to the ventral nerve cord to synapse with motor circuit neurons (White et al., 1986). Higher order PVD branches were annotated in some EM sections but were not initially recognized as emanating from PVD (Albeg et al., 2011; Hall and Treinin, 2011; Oren-Suissa et al., 2010). Immunostaining for the acetylcholine receptor (AChR) receptor subunit, DEG-3, provided the first glimpse of the elaborate web of lateral PVD branches (Halevi et al., 2002; Yassin et al., 2002) that was later confirmed with GFP

* Corresponding author.
E-mail address: david.miller@vanderbilt.edu (D.M. Miller).

https://doi.org/10.1016/j.ydbio.2019.04.002
Received 31 October 2018; Received in revised form 9 March 2019; Accepted 5 April 2019
Available online 17 April 2019

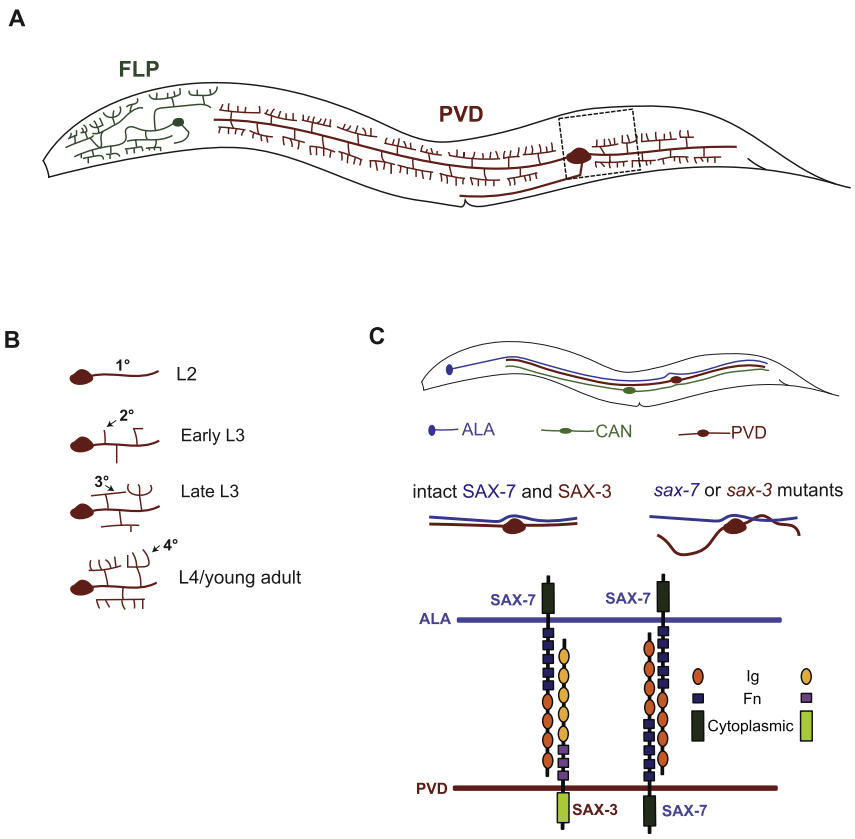

Fig. 1. PVD dendritic branching and fasciculation with a neighboring neuron. (A) Tracings of PVD (red) and FLP (green) along the body of the worm, anterior to left, ventral down. (B) Post embryonic development of PVD dendrites during successive L2, L3 and L4 larval stages. (C) The PVD 1^0 dendrite is located in the lateral nerve cord with ALA and CAN neurons. In the wild type, the PVD 1^0 dendrite fasciculates with ALA and throughout its length. In *sax-7* and *sax-3* mutants, the PVD 1^0 dendrite fails to fasciculate with ALA. SAX-7 in ALA and SAX-3 in PVD interact through their extracellular domains to facilitate fasciculation of ALA with the PVD 1^0 dendrite. SAX-7 may also mediate additional homophilic interactions between PVD and ALA.

markers (Tsalik et al., 2003; Watson et al., 2008). Each lateral or 2^0 PVD branch is tipped with an array of terminal dendritic processes that together constitute a repetitive motif or "menorah," each rooted in the 1° dendrite, that defines the PVD arbor (Oren-Suissa et al., 2010). This dendritic architecture is generated by a series of orthogonal branching events that occur during larval development (Oren-Suissa et al., 2010; Smith et al., 2010).

3. Developmentally regulated branching morphogenesis gives rise to the PVD dendritic arbor

Each PVD neuron arises during the second larva stage (L2) from the stereotypical division of postembryonic ectodermal cells (V5R and V5L) that also generates the postdeirid, a somatosensory organ that contains PVD, the PDE dopaminergic mechanosensory neuron and two accessory support cells (Sulston and Horvitz, 1977) (Fig. 6A). The subsequent appearance of PVD neurites has been tracked in detail by live-cell imaging (O. W. Liu and Shen, 2011; Smith et al., 2010). PVD is especially suitable for this approach because of its external location directly beneath the transparent cuticle and because PVD morphogenesis occurs during larval development when *C. elegans* is readily accessible for imaging studies. The PVD axon appears first, followed by the 1^0 dendrites, which grow out in close apposition to a pre-existing lateral nerve cord (Fig. 1B). Next, filopodia projecting in either dorsal or ventral directions from the 1^0 dendrite are observed during the late L2/early L3 larval period. Filopodia show active cycles of extension and retraction with a subset eventually stabilizing as 2^0 dendrites as they reach an axial boundary at the medial edge of body muscle cells. At this position, each 2^0 dendrite makes a 90^0 turn to project in either the anterior or posterior direction as a 3^0 dendrite. Typically, an additional 3^0 dendrite emerges from the branch point to grow out in the opposite direction, effectively "crossing the T" for each 2^0 dendrite (Fig. 1B). 3^0 dendrites continue outgrowth until contacting the tip of an adjacent 3^0 branch approaching from the opposite direction. A self-avoidance response then ensues with multiple rounds of mutual contact and retraction until each 3^0 branch eventually adopts a right angle turn to leave a gap between adjacent menorahs and give rise to a 4^0 dendrite (Fig. 1B) (Smith et al., 2010). In a pattern resembling that of 2^0 branches, additional 4^0 dendrites emerge in the L4 stage as saltatory filopodia that exit the lateral edge of each 3^0 dendrite to insinuate themselves within the narrow space separating the overlying skin from muscle cells underneath. 4^0 branch outgrowth terminates at adjacent dorsal and ventral nerve cords. FLP neuron morphogenesis displays a similar dendritic arbor and pattern of outgrowth (Albeg et al., 2011; Smith et al., 2010).

Molecular mechanisms that define the stereotypical architecture of the PVD dendritic arbor are diverse and involve a combination of external cues and intrinsic pathways that drive branching outgrowth and trajectory (Dong et al., 2015). We will use the sequential appearance of PVD branches as a framework for reviewing our current understanding of these mechanisms.

4. Fasciculation with the ALA axon steers outgrowth of the PVD primary dendrite

Beginning in the L2 larval stage, PVD 1^0 dendrites initiate outgrowth along a pre-existing lateral nerve cord containing processes from the ALA and CAN neurons as well as a tube-like extension of the excretory cell (Smith et al., 2010; White et al., 1986) (Fig. 1C). While this close proximity is suggestive of interaction between the 1^0 PVD dendrite and the ALA and CAN axons (Smith et al., 2010), until recently, this relationship was unexplored. High-resolution imaging has now shown that the PVD 1^0 dendrite fasciculates with ALA but not CAN (Chen et al., 2019; Ramirez-Suarez et al., 2019). A necessary role for neuron-specific interactions with ALA is consistent with the finding that ablation of ALA results in a misguided PVD 1^0 dendrite whereas selective perturbation of CAN outgrowth does not. The importance of ALA as a guidepost for steering PVD outgrowth is underscored by the finding that mutations that disrupt UNC-6/Netrin pathway signaling or indirectly alter the placement of the

PVD 1^0 dendrite by perturbing ALA outgrowth (Ramirez-Suarez et al., 2019). A candidate gene approach, based on neuron-specific expression profiling of PVD and ALA (Nath et al., 2016; Smith et al., 2010), determined that the membrane proteins SAX-7/L1CAM and SAX-3/Robo interact to mediate PVD fasciculation with ALA (Fig. 1C) (Chen et al., 2019). *sax-7* mutants perturb PVD fasciculation with ALA. Although SAX-7/L1CAM is expressed in both PVD and ALA, selective expression of wild-type *sax-7* in ALA but not PVD at least partially rescues the Sax-7 defasciculation defect (Chen et al., 2019; Ramirez-Suarez et al., 2019). Similar experiments confirmed that the Robo receptor, SAX-3, is specifically required in PVD to maintain normal outgrowth of the primary dendrites (Chen et al., 2019). Immunoprecipitation and cell aggregation experiments demonstrated that SAX-7 physically interacts with SAX-3 (Chen et al., 2019). Although the secreted protein Slit functions as the canonical ligand for Robo receptors including SAX-3 (Hao et al., 2001), mutations that disrupt the *C. elegans* Slit locus, *slt-1*, do not perturb placement of PVD 1^0 dendrites. Thus, these results indicate that SAX-7/L1CAM functions in ALA as a novel ligand for the SAX-3/Robo receptor in PVD and that this interaction is required for normal outgrowth of PVD 1^0 dendrites along the ALA axon (Fig. 1C) (Chen et al., 2019). This defect is correlated with the altered shape and dynamics of a growth cone-like structure on developing PVD 1^0 dendrites. In the wild type, the tip of the PVD 1^0 dendrite remains compact whereas it expands and shows slower outgrowth and frequent lateral filopodial protrusions in *sax-3* and *sax-7* mutants. Actin dynamics at the tip is also perturbed in *sax-3* and *sax-7* mutants. Together, these results suggest that SAX-7/L1CAM interaction with SAX-3/Robo regulates the actin cytoskeleton in the PVD 1^0 dendrite to maintain outgrowth along the ALA axon tract. The necessary role for the SAX-3 intracellular domain in this mechanism (Chen et al., 2019) and the established function of Robo receptors in regulating actin dynamics (McConnell et al., 2016) are consistent with this idea. In addition to providing a molecular mechanism for the precise outgrowth of the PVD 1^0 dendrites, this work also represents a new model for how these conserved cell surface proteins, L1CAM and Robo, might steer dendrite outgrowth in more complex nervous systems by fasciculation with axons. Further investigation in *C. elegans* should reveal additional components of this pathway. For example, the misrouting of the PVD 1^0 dendrite is more severe in *sax-7* than in *sax-3* mutants which suggests that SAX-7 could also interact with another cell surface component in PVD to steer dendrite outgrowth. Notably, rescue of the Sax-7 defasciculation defect by expression of SAX-7 in ALA, is significantly enhanced by co-expression of SAX-7 in PVD, thus suggesting that homophilic interactions between SAX-7 in ALA and in PVD could also promote fasciculation with ALA (Ramirez-Suarez et al., 2019) (Fig. 1C). PVD dendrite trajectory along the body axis is maintained in *sax-7* and *sax-3* mutants which suggests that an additional signaling pathway may direct outgrowth in the anterior and posterior directions. Finally, additional genetic evidence indicates that outgrowth of the PVD 1^0 dendrite depends on interaction of the DMA-1 receptor complex in PVD with its ligands in ALA (i.e., SAX-7, MNR-1) (Ramirez-Suarez et al., 2019) (O. W. Liu and Shen, 2011) (see below). For example, in addition to defective ALA-PVD fasciculation, the PVD 1^0 dendrite is also truncated in *sax-7* mutants. This effect is particularly acute for the posteriorly directed 1^0 dendrite. Interestingly, ALA-PVD fasciculation does not depend on SAX-7 interactions with DMA-1 (Ramirez-Suarez et al., 2019). Thus, SAX-7 in ALA appears to interact with separate receptors in PVD for fasciculation (i.e., SAX-3) vs growth (i.e., DMA-1) of the PVD 1^0 dendrite (Chen et al., 2019; Ramirez-Suarez et al., 2019). It will be interesting to determine if preferential effect of the DMA-1-dependent pathway mutation on the posterior 1^0 dendrite is related to its unique microtubule polarity (i.e., + end out, see below) (Taylor et al., 2015) or the recent observation that the posterior 1^0 dendrite is severely curtailed in *mec-3* mutants (O'Brien et al., 2017).

5. A multicomponent receptor-ligand complex regulates PVD dendritic branching

The ready visibility of the PVD arbor labeled with GFP markers has been extensively utilized in genetic screens to identify new regulators of PVD branching. This strategy is particularly powerful in *C. elegans* because mutant effects can be easily detected by direct inspection of live animals (Dong et al., 2013; Salzberg et al., 2013; Smith et al., 2010). In an early example of this approach, a mutation in the *dma-1* locus dramatically reduced the number and lengths of PVD 2^0 dendrites and virtually eliminated higher order 3^0 and 4^0 branches. DMA-1 encodes a transmembrane protein with extracellular Leucine Rich Repeat (LRR) domains. DMA-1 functions in PVD as a cell surface receptor that responds to external cues to direct branch outgrowth (O. W. Liu and Shen, 2011) (Fig. 2A and B). A comprehensive model of DMA-1 function in PVD branching derives from subsequent genetic studies that revealed an additional component of the DMA-1 receptor complex and its ligands, a pathway for modulating temporal DMA-1 expression and downstream effectors that interact with the PVD actin cytoskeleton (Díaz-Balzac et al., 2016; Dong et al., 2013, 2016; Salzberg et al., 2013, 2014; Smith et al., 2013; Zou et al., 2018, 2016) (Fig. 2).

Mutations in the membrane proteins SAX-7/L1CAM and MNR-1/Menorin revealed a key role for the epidermis in patterning PVD dendritic morphology (Dong et al., 2013; Salzberg et al., 2013). *sax-7* and *mnr-1* show highly similar mutant phenotypes, in which the repeating array of dendritic menorahs is replaced with a disorganized web of lateral branches (Fig. 2A). The PVD dendritic arbor is closely apposed to the skin (aka “hypodermis” due to its location beneath the extracellular cuticle), a location that mirrors that of sensory neurons in *Drosophila* and mammals (Fig. 3A) (Abraira et al., 2017; Albeg et al., 2011; Y. N. Jan and L. Y. Jan 2010). Normally, SAX-7 and MNR-1 are expressed in the epidermis to pattern PVD dendrite outgrowth. As a homolog of the L1CAM family of membrane proteins, SAX-7 is predicted to function as an adhesion protein (Chen and Zhou, 2010) and in this case, displays a striking pattern of localization on the epidermis that mimics key structural features of each PVD menorah (Fig. 3B). Axial bands of SAX-7 protein coincide with the lateral location of 3^0 dendrites and additional offshoots of thin, orthogonal SAX-7 stripes parallel the trajectory of 4^0 dendrites. MNR-1 is also expressed in the skin but is more broadly distributed. Genetic and biochemical data are consistent with a model which both SAX-7 and MNR-1 are required for direct interactions with the DMA-1 receptor to pattern PVD dendritic outgrowth (Dong et al., 2013; Salzberg et al., 2013). For example, ectopic expression of MNR-1 in body muscle cells induces adjacent arrays of dendritic branches resembling that of a baobab tree. Genetic epistasis experiments have shown that both SAX-7 and DMA-1 are necessary for the baobab phenotype (Salzberg et al., 2013). In addition, all three components (DMA-1, SAX-7 and MNR-1) are required for co-immunoprecipitation from cultured cells (Dong et al., 2013). Based on these results, placement of PVD 3^0 and 4^0 branches is proposed to arise from dendritic outgrowth directed by an epidermal path paved with SAX-7 and MNR-1 that interact with the DMA-1 receptor in PVD (Fig. 2B). Although all of these components are conserved, their interactions governing dendrite outgrowth are novel. SAX-7 and other members of the L1CAM family mediate homophilic adhesion between extracellular Immunoglobulin (Ig) domains (Pocock et al., 2008). In this case, however, the Fibronectin type III domains (FNIII) are required for heterophilic interaction with the LRR region of DMA-1 (Fig. 2B). MNR-1 contains a single transmembrane domain and an extracellular sequence previously described as a domain of unknown function (DUF2181) that define the widely conserved Fam151 family of proteins (Dong et al., 2013; Salzberg et al., 2013).

More recent genetic screens have revealed an additional component of the DMA-1 receptor-ligand complex (O'Brien et al., 2016). Mutations that disrupt the *lect-2* gene produce PVD branching defects virtually identical to those of *sax-7* and *mnr-1* (Fig. 2A). Moreover, the PVD branching phenotypes of *lect-2; sax-7* and *lect-2;mnr-1* double mutants are

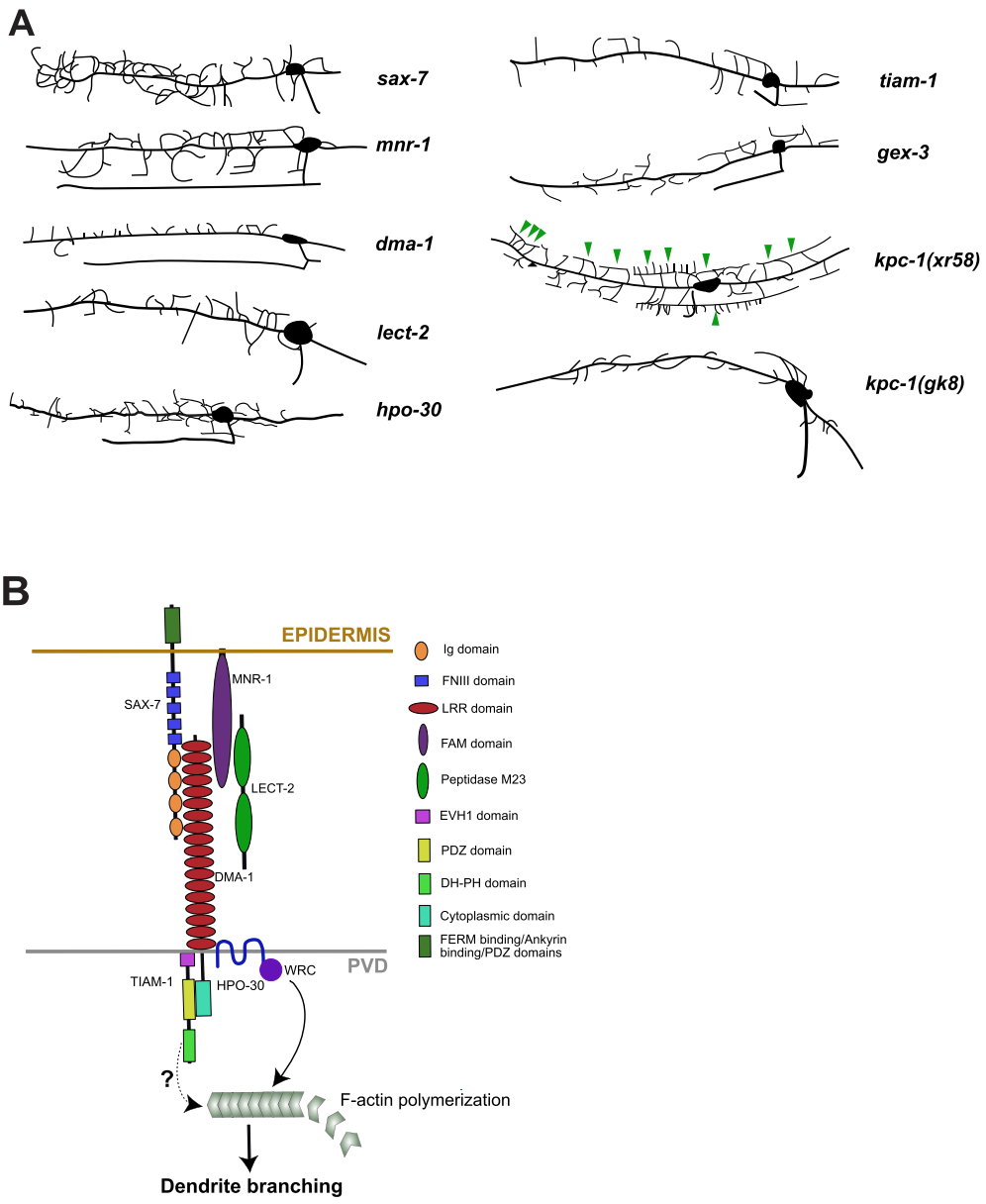

Fig. 2. The DMA-1 receptor complex promotes PVD branching. (A) Tracing of disrupted PVD dendrite branching in various mutant backgrounds. Self-avoidance defects are indicated by green arrowheads. Alleles are *sax-7(nj48)*, *mnr-1(wy758)*, *dma-1(wy686)*, *lect-2(wy953)*, *tiam-1(tm1556)*, *gex-3(zu196)*, *kpc-1(gk8)* (null allele) and *kpc-1(xr58)* (hypomorphic allele), (B) Receptor complex (DMA-1, SAX-7, MNR-1, LECT-2, HPO-30) that mediates PVD interaction with the epidermis and downstream effectors, TIAM-1 and the WRC (Wave-Regulatory Complex), that direct F-actin polymerization.

no more severe which suggests that all of these components function in a common genetic pathway. *lect-2* is highly expressed in body muscle and encodes a secreted protein that decorates selected nerve tracts. Strikingly, extracellular localization of GFP-tagged LECT-2 also coincides with the SAX-7 stripes on the epidermis (Fig. 3B) that pattern 3^0 and 4^0 branch outgrowth and this effect is eliminated in *sax-7* mutants (Díaz-Balzac et al., 2016; Zou et al., 2016). Interactions between SAX-7 and LECT-2 were confirmed with biochemical pull-down experiments which also showed that LECT-2 enhanced the overall binding affinity of the DMA-1, SAX-7 and MNR-1 receptor-ligand complex. Together, these results suggest that LECT-2 functions as a soluble ligand that strengthens DMA-1 binding to SAX-7 and MNR-1 on the epidermal surface (Fig. 2B). Additional experiments suggest that this role for LECT-2 may be especially important for terminal 4^0 branch elongation. Selective elimination of LECT-2 expression from body muscles disrupted outgrowth of adjacent 4^0 dendrites but not 2^0 and 3^0 branches. The obverse condition of restricting LECT-2 expression to a single body muscle cell rescues all 2^0 and 3^0 dendrites but selectively restores only nearby 4^0 branches (Zou et al., 2016). Together these findings suggest that LECT-2 functions effectively as a "permissive" cue but that higher local concentrations of LECT-2 may be necessary for the normal extension of 4^0 branches (Díaz-Balzac et al., 2016; Zou et al., 2016). This idea is consistent with the additional finding that artificial over-expression of LECT-2 from other cell types is sufficient to fully rescue PVD branching in a *lect-2* mutant (Díaz-Balzac et al., 2016). The LECT-2 protein contains an evolutionarily ancient M23 domain found in prokaryotic proteases that digest peptidoglycans in bacterial cell walls. A closely related mammalian LECT2 protein (leukocyte cell-derived chemotaxin-2) was first described as an attractive factor for neutrophils but is also an important biomarker and potential therapeutic target for several human pathologies (Slowik and Apte, 2017; Yamagoe and Mizuno, 1996). A recent report also suggests that LECT2 may promote dendritic outgrowth in mice (Ohtomi, 2010). Thus, these studies in *C. elegans* may have revealed new modes of molecular interactions to shape cell adhesion and dendrite morphogenesis that may also illuminate similar core mechanisms in more complex organisms.

6. Regulated surface expression of the DMA-1 receptor controls dendrite outgrowth

In addition to nascent outgrowth, the step-wise elaboration of the

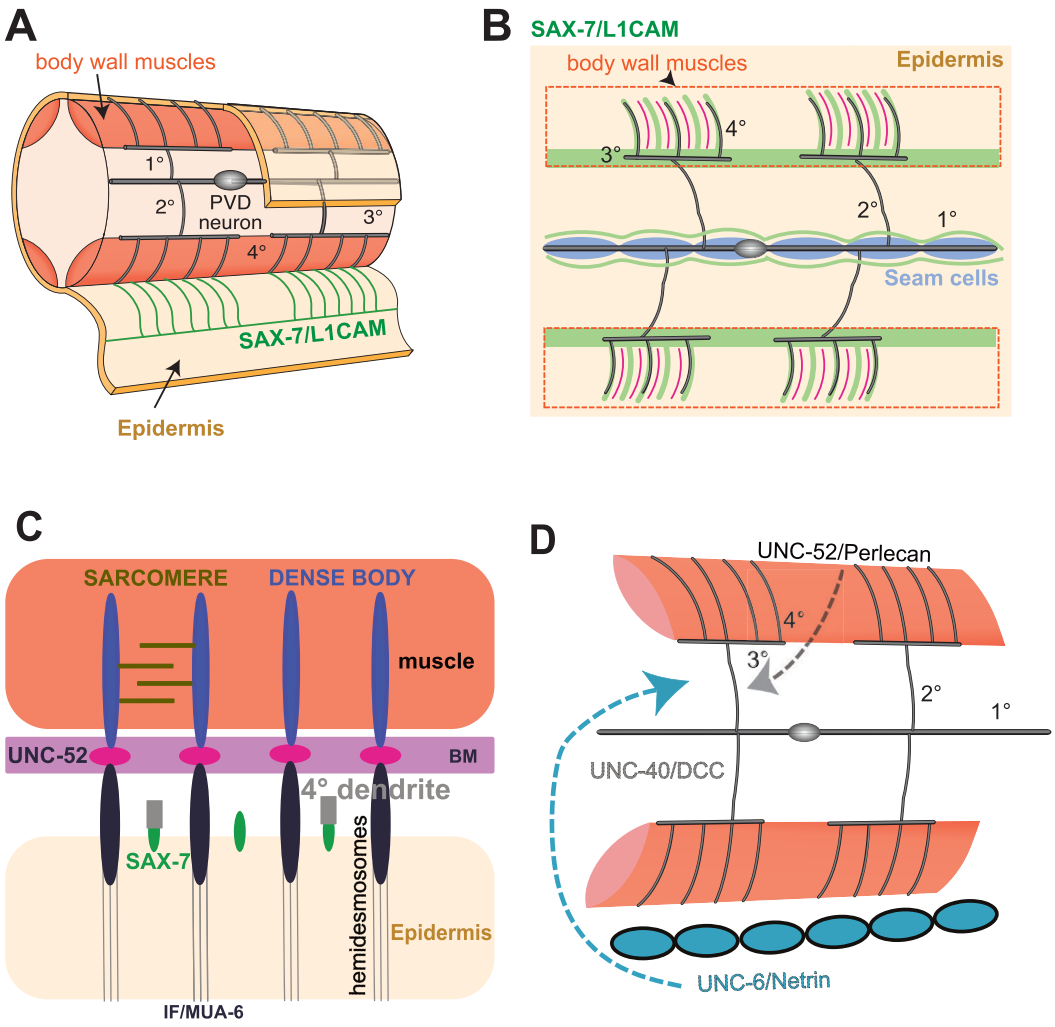

Fig. 3. Regions of expression for proteins involved in dendrite morphogenesis. (A) Cut-away of the PVD neuron with 4^0 dendrites sandwiched between body-wall muscles and the epidermis. PVD dendrites grow out on the inner surface of the skin with 4^0 branches aligned with SAX-7/L1CAM stripes (green) adjacent to underlying body muscles. Adapted from O'Brien et al. (2016). (B) SAX-7/L1CAM (green) is localized in narrow bands flanking seam cells, in bilateral longitudinal stripes beneath 3^0 dendrites and in circumferential lines adjacent to body muscle cells. UNC-52/Perlecan (pink) is localized to the body wall muscles and is denoted by stripes between the PVD 4° dendrites. Dashed lines outline the location of body muscle cells (C) Schematic depicting PVD 4^0 dendrites and location of SAX-7/L1CAM in conjunction with the basement membrane (BM) and body muscles. UNC-52/Perlecan is expressed in body muscle cells and localized to the basement membrane where it links muscle dense bodies to intermediate filaments (IF/MUA-6) anchored in the epidermis. Adapted from Liang et al. (2015). (D) PVD 2^0 dendrite outgrowth depends on soluble cues UNC-52/Perlecan (from muscle) and UNC-6/Netin from ventrally located cells and cell-autonomous UNC-40/DCC function in PVD.

PVD arbor also depends on the orthogonal redirection of the tips of existing dendrites as they are extending. For example, 3^0 dendrites grow out on the epidermis aligned with a longitudinal path paved with SAX-7 (Fig. 3B). Although the SAX-7 label is apparently uniform throughout the length of the PVD arbor, 3^0 dendrites eventually adopt a right angle turn to exit the longitudinal SAX-7 stripe and grow along SAX-7-marked lines adjacent to body muscles (Liang et al., 2015) (see below). A forward genetic screen revealed a key regulator of PVD morphogenesis that is required for this orthogonal turn and for mediating an earlier interaction with a different SAX-7 landmark. Both the PVD and FLP arbors are highly disrupted by mutations in the *kpc-1* locus (Dong et al., 2016; Salzberg et al., 2014; Schroeder et al., 2013). Null alleles of *kpc-1* display a distinctive phenotype in which PVD lateral branches appear "trapped" within a region surrounding the 1^0 dendrite and PVD soma (Fig. 2A). Notably, this zone corresponds to the location of an additional SAX-7 boundary that borders the outside edge of a longitudinal array of epidermal seam cells that flanks the 1^0 dendrite. 2^0 dendrites normally traverse this region to reach the more distal sublateral SAX-7 stripes (Fig. 3B). Additional experiments suggest that *kpc-1* down-regulates adhesion to SAX-7 for this transit. Lateral dendritic outgrowth is disordered but expands beyond the seam cell boundary in double mutants of *kpc-1* with either *sax-7* or *mnr-1* thus suggesting SAX-7 and MNR-1 are required for "trapping" 2^0 dendrites adjacent to seam cells in *kpc-1* mutants. In a dramatic demonstration of the role of SAX-7 in mediating the Kpc-1 phenotype, forced expression of MNR-1 and SAX-7 in laterally placed touch neurons in a *kpc-1;sax-7* mutant resulted in the ectopic fasciculation of PVD branches with touch neuron processes. These results suggest that KPC-1 normally functions to antagonize PVD interactions with SAX-7 landmarks (Dong et al., 2016). This mechanism apparently involves *kpc-1*-dependent down-regulation of DMA-1 surface expression in PVD (Fig. 4C). Several lines of evidence are consistent with this model. First, over-expression of DMA-1 in PVD mimics branching defects observed in *kpc-1* mutants. Second, *dma-1;kpc-1* double mutants show the Dma-1 phenotype (i.e., truncated 2^0 branches) but not the "trapped" array of lateral branches observed in *kpc-1*, a result suggesting that DMA-1 is required for this *kpc-1* defect (Fig. 2B). Third, DMA-1 protein levels are elevated in *kpc-1* mutants. Fourth, a substantial fraction of GFP-tagged DMA-1 co-localizes with a late endosome/lysosome marker in the wild type but largely resides at the PVD cell surface in *kpc-1* mutants. This finding suggests that KPC-1 normally shuttles DMA-1 to the

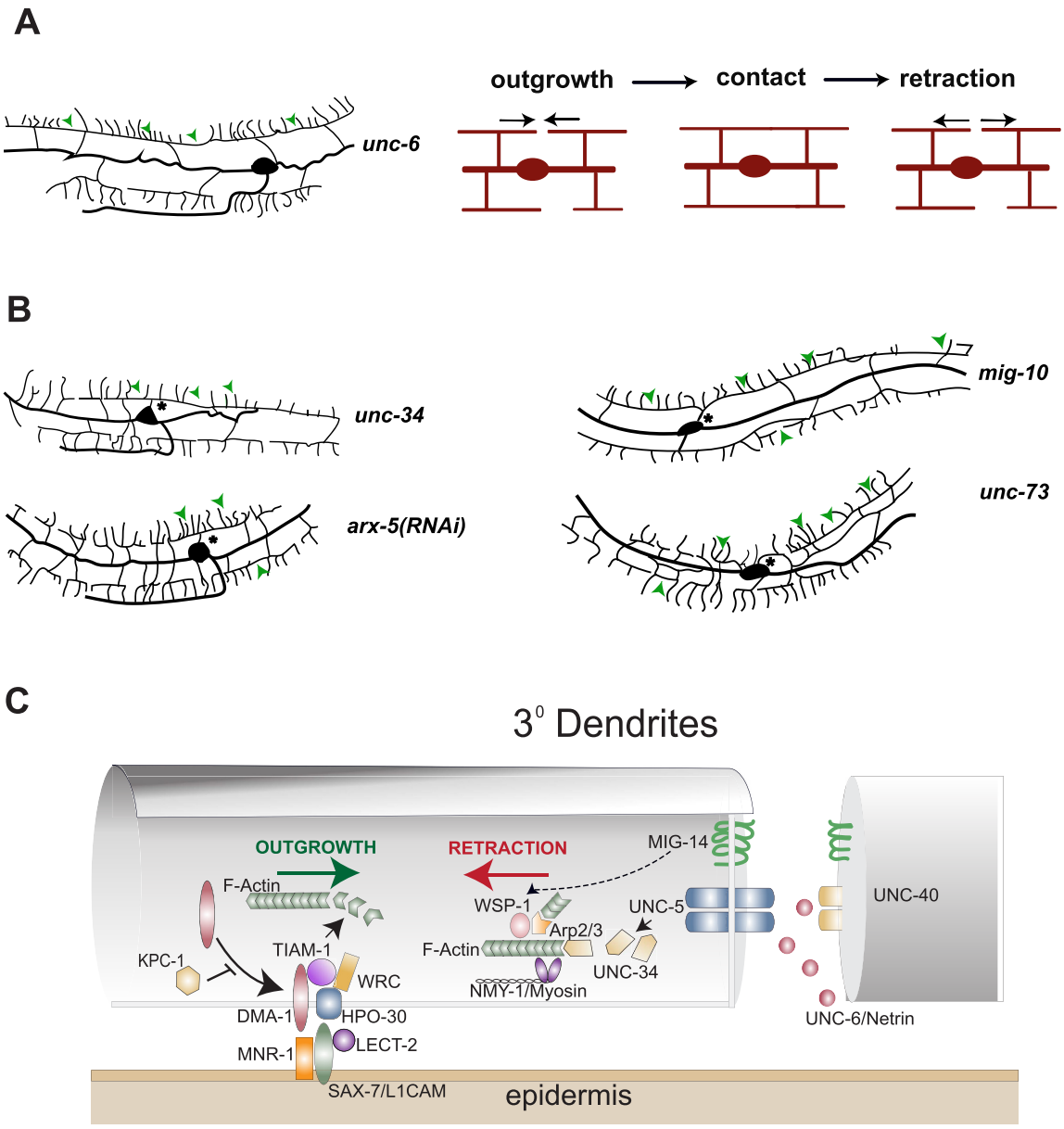

Fig. 4. Opposing pathways promote actin polymerization to define dendrite length. (A) Representative tracings of PVD morphology in an *unc-6(ev400)* background and a cartoon summarizing self-avoidance in 3° PVD dendrites denoting growth, contact and retraction. (B) Representative tracings of PVD morphology for mutants of genes that encode regulators of actin polymerization (UNC-34/ENA/VASP, MIG-10/Lamellipodin, UNC-73/Trio) and for RNAi of Arp2/3 complex component, ARX-5/p21. Alleles are *unc-34(gm104)*, *mig-10(ct41)* and *unc-73(rh40)*. Arrowheads denote self-avoidance defects. (C) Model showing components for 3^0 branch outgrowth vs retraction. KPC-1 antagonizes surface expression of DMA-1 which interacts with epidermal membrane-associated proteins, SAX-7/L1CAM and MNR-1, and the soluble ligand LECT-2 to function with HPO-30 to promote actin polymerization and dendrite outgrowth via TIAM-1 and the WRC (WAVE Regulatory Complex). UNC-6/Netrin is captured by UNC-40/DCC for interaction with UNC-5 and activation of UNC-34/Ena/VASP which functions with WSP-1/WASP and the Arp2/3 complex to drive F-actin assembly for NMY-1/myosin-dependent dendrite retraction in the self-avoidance response. UNC-73/Trio and MIG-10/Lamellipodin are not shown. Homophilic MIG-14/Wntless interaction also mediates self-avoidance.

lysosome for degradation to prevent interaction with SAX-7 at the PVD surface. Although the KPC-1 protein is a member of the furin family of proprotein convertases, its protease activity is selectively required for self-activation but does not apparently cleave DMA-1 (Dong et al., 2016). Instead, KPC-1 physically interacts with the DMA-1 extracellular domain for shuttling it to the lysosome, a mechanism paralleling that of a mammalian convertase, PCSK9, that binds to the extracellular EGF domain of the LDL receptor to mediate its degradation (Poirier and Mayer, 2013). Because PVD branches sequentially enter and then exit distinct SAX-7-labeled regions during outgrowth, its seems likely that the surface abundance of DMA-1 must be temporally regulated by *kpc-1* as the PVD arbor emerges. How such a mechanism might work, however, has not been determined.

7. Patterning SAX-7 stripes on the epidermis

Given the instructive role of SAX-7 in sculpting PVD, pathways that direct the placement of SAX-7 to discrete locations on the epidermis should be crucially important to shaping PVD dendrite morphology. A forward genetic screen for PVD morphological defects implicated two molecularly distinct components, the membrane protein and fusogen, EFF-1 and the dynein motor complex in SAX-7 localization (Zhu et al., 2017). PVD branching is disordered and highly exuberant in *eff-1* mutants in which the regular array of menorahs is disrupted and numerous

ectopic branches emerge (Oren-Suissa et al., 2010; Zhu et al., 2017). This Eff-1 phenotype is correlated with the misplacement of SAX-7 in the epidermis which could arise from the failure of epidermal cell fusion that EFF-1 normally mediates in the embryo to produce the post-larval epidermal syncytium (Mohler et al., 2002; Zhu et al., 2017). Indeed, misplaced PVD branches are typically aligned with the edges of unfused epidermal cell in *eff-1* mutants. Although earlier work reported that EFF-1 functions in PVD to control dendritic morphogenesis (Oren-Suissa et al., 2010), more recent evidence shows that EFF-1 is selectively required in the epidermis (Zhu et al., 2017). A second hit from this screen detected a mutation in *dli-1* which encodes the dynein light intermediate chain and component of the dynein minus-end motor complex (Zhu et al., 2017). *dli-1* mutants show disordered and ectopic PVD branches resembling that of *eff-1* mutants that is also correlated with the misplacement of SAX-7. Rescue experiments confirmed that DLI-1 function is required in the epidermis to restore normal PVD morphology and could therefore mediate epidermal cell fusion although this possibility was not directly investigated. The *dli-1* mutant also shows a second striking phenotype in which the anterior region of the PVD arbor shows a dramatically reduced number of complete menorahs (Zhu et al., 2017). In this case, dynein function is cell autonomous for PVD, as previously reported (Aguirre-Chen et al., 2011), likely because dynein is required to traffic branching components to the microtubule minus end which is oriented toward the tip of the anteriorly directed 1^0 dendrite (see below) (Taylor et al., 2015; Zhu et al., 2017).

In addition to defining sublateral longitudinal stripes that pattern 3^0 branch outgrowth, SAX-7 is also localized to circumferential bands that coincide with the long axis of 4^0 dendrites in their location sandwiched between body muscles and the epidermis (Fig. 3B and C). Recent results suggest that the striking periodic pattern of SAX-7 localization is defined by repetitive arrays of structural components in adjacent muscle cells (Liang et al., 2015). In *C. elegans*, body muscles are firmly attached to the skin which is deformed by muscle contraction to drive locomotion. Each muscle sarcomere, the basic contractive unit, is anchored to medial M-lines and orthogonal dense body structures at each end. The heparan sulfate proteoglycan and extracellular matrix protein UNC-52/perlecan is positioned in the basement membrane to link each M-line and dense body to tight junctions or hemidesmosomes in the epidermis (Fig. 3C) (Moerman and Williams, 2006). The SAX-7 stripes are located in parallel to produce alternating bands of SAX-7 vs UNC-52-containing bridges between muscle and skin (Fig. 3B and C). SAX-7 localization also complements that of a key structural component of the hemidesmosomes, the intermediate filament protein, MUA-6. The periodic pattern of SAX-7 stripes and 4^0 branch outgrowth is severely disrupted in either *unc-52* or *mua-1* mutants. Because muscle sarcomeres are assembled prior to the localization of SAX-7 to the epidermis, these results suggest that muscle attachments to the skin are responsible for patterning the SAX-7 stripes. The cellular mechanism of this effect is unclear but it may depend on the SAX-7 cytoplasmic domain (Liang et al., 2015). The precise placement of 4^0 dendrites relative to the underlying muscle structure could be physiologically important because PVD has been proposed to function as a proprioceptor that monitors the contractile state of body muscles to modulate posture (Albeg et al., 2011). It should be noted that the Bulow lab recently reported different results suggesting that neither epidermal structure nor 4^0 branch elongation are perturbed in *unc-52* mutants but that 2^0 branch outgrowth is curtailed (see below) (Celestrin et al., 2018) (Fig. 3D).

8. Additional extrinsic dendritic patterning components

Although PVD branch outgrowth clearly depends on the SAX-7 ligand-receptor complex (Fig. 2A and B), genetic evidence suggests that additional external cues are required to shape the PVD dendritic arbor. Of particular note is the observation that mutations that disrupt the DMA-1 receptor result in shorter lateral branches than observed in mutants for its ligands, SAX-7, MNR-1 and LECT-2 (Fig. 2A). Moreover, *dma-1* is epistatic to *sax-7*, *mnr-1* and *lect-2*, which indicates that the longer dendrites observed in single mutants of *sax-7*, *mnr-1* and *lect-2* depend on DMA-1 (Díaz-Balzac et al., 2016; Dong et al., 2013; Salzberg et al., 2013; Zou et al., 2016) and therefore are suggestive of additional epidermal ligands that promote DMA-1-dependent dendritic growth.

A second clue indicative of additional external cues for patterning PVD dendrites is the recent finding that the receptor tyrosine phosphatase, CLR-1, functions in parallel to SAX-7 in the epidermis to promote PVD branch outgrowth (X. Liu et al., 2016). PVD branching is impaired in *clr-1* mutants with the strongest effect on 4^0 dendrites which initiate outgrowth on the circumferential SAX-7 stripes but rarely extend to wild-type length. Overall PVD outgrowth is severely curtailed in *clr-1* double mutants with *sax-7*, *dma-1* and *mnr-1* in which all PVD branches including the 1^0 dendrite are much shorter and more disordered than in any of the single mutants. Although CLR-1 contains extracellular Ig and FNIII motifs, only the CLR-1 cytoplasmic phosphatase domain is essential to its role in dendrite outgrowth. This finding suggests that CLR-1 likely dephosphorylates a cytoplasmic target in the epidermis that is necessary for PVD dendrite outgrowth. The downstream effector in this case is unknown. Potential disruption of overall epidermal morphogenesis and structure in a *clr-1* mutant might also contribute to the PVD branching defect but this possibility was not investigated (X. Liu et al., 2016).

Recent evidence suggests that extracellular matrix components originating from body muscle may function in concert with UNC-6/Netrin to promote 2^0 branch outgrowth (Celestrin et al., 2018) (Fig. 3D). The *unc-52(ra515)* deletion allele selectively removes four specific Ig domains from UNC-52/Perlecan and results in fewer 2^0 branches but otherwise does not perturb 3^0 or 4^0 branch morphogenesis. *unc-52(ra515)* animals also show normal muscle structure but reduced localization of the extracellular matrix protein, NID-1/nidogen, to muscle dense body structures. A *nid-1/nidogen* loss-of-function mutant phenocopies the PVD 2^0 branch outgrowth defect of *unc-52(ra515)*. Together, these results suggest that specific UNC-52 Ig domains are required for interactions with NID-1/Nidogen in the basal lamina to promote 2^0 branch outgrowth. Additional genetic results confirmed that UNC-6/Netrin and its receptor UNC-40/DCC are also required for the wild-type complement of 2^0 branches (Smith et al., 2010) and function in a common pathway with UNC-52/Perlecan and NID-1/Nidogen (Celestrin et al., 2018). UNC-6/Netrin is secreted from ventrally-positioned cells to direct the dorsal trajectory of motor neuron axons by interacting with the UNC-40/DCC receptor (Wadsworth, 2002). However, PVD-specific expression of UNC-40/DCC rescues PVD 2^0 branching defects suggesting that UNC-40/DCC may drive 2^0 branch outgrowth by responding to an UNC-6/Netrin signal anchored to the basal lamina by UNC-52/Perlecan and NID-1/Nidogen (Celestrin et al., 2018). The mechanism of this effect must depend on UNC-52 functioning at a distance from body muscles because 2^0 branches grow out along the epidermis in medial domains that are not adjacent to laterally placed body muscles (Albeg et al., 2011) (Fig. 3A). It should be noted that a different role for UNC-52 function in 4^0 branch outgrowth was reported by the Shen lab (see above) (Liang et al., 2015). The reasons for these disparate results are unclear.

9. How does the DMA-1 receptor complex guide dendrite outgrowth?

The crucial role of the cytoskeleton in dendrite outgrowth is well-established and thus would also be expected to drive PVD morphogenesis (Delandre et al., 2016; Y. N. Jan and L. Y. Jan 2010; Luo, 2002). Microtubules (MTs) are prominently localized to the PVD axon and 1^0 dendrite (Harterink et al., 2018; Maniar et al., 2011; Richardson et al., 2014; Sundararajan et al., 2018; L. T. Tang et al., 2019; Taylor et al., 2015) and mutations that alter MT organization and polarity disrupt PVD morphology (see below).

Recent work has shown that PVD morphogenesis also depends on the actin cytoskeleton and its interactions with the DMA-1 receptor-ligand

complex (L. T. Tang et al., 2019; Zou et al., 2018). Actin monomers (G-actin) can be rapidly assembled into filamentous structures (F-actin) which can also be dissociated to produce G-actin for new rounds of assembly. The ancient origin of this cytoskeletal component is underscored by the strong conservation of the actin amino sequence and the large number of specialized accessory proteins that control actin cytoskeletal dynamics (Pollard, 2016). Imaging with live-cell fluorescent markers for F-actin has detected strong enrichment in the 1^0 dendrite and at the tips of growing lateral branches throughout development (Liao et al., 2018; Sundararajan et al., 2018; L. T. Tang et al., 2019; Zou et al., 2018). A necessary role for actin in PVD dendrite morphogenesis is convincingly demonstrated by mutations in the actin encoding gene, *act-4*, which disrupt PVD lateral branching (L. T. Tang et al., 2019; Zou et al., 2018). Genetic analysis also detected strong PVD branching defects for mutations in conserved regulators of actin assembly. Rho family GTPases modulate actin dynamics and are themselves activated by Guanine Exchange Factors or GEFs. A mutation in one of these GEFs, TIAM-1 (T-lymphoma invasion and metastasis-inducing protein-1) impairs PVD lateral branching (Fig. 2A) (L. T. Tang et al., 2019; Zou et al., 2018). Multiple lines of evidence suggest that the DMA-1 receptor interacts with TIAM-1 to direct PVD lateral branching. First, the removal of a four amino acid PDZ binding motif at the cytoplasmic C-terminus of DMA-1 (DMA-1Δ4AA) disrupts binding to the canonical PDZ domain of TIAM-1 (L. T. Tang et al., 2019; Zou et al., 2018). Second, the *in vivo* significance of this interaction is validated by an experiment with a chimeric protein in which TIAM-1 is fused to a DMA-1 protein lacking its intracellular domain (DMA-1Δ4AA) is sufficient to restore higher order branching to a *dma-1* mutant whereas DMA-1ΔICD (intracellular domain) alone is not (Zou et al., 2018). Thus, these results indicate that DMA-1 drives dendrite outgrowth by interacting with TIAM-1/GEF to promote actin assembly.

Additional evidence, however, suggests that a new component of the DMA-1 receptor complex, HPO-30, is also required for mediating interactions with the actin cytoskeleton (L. T. Tang et al., 2019; Zou et al., 2018). *hpo-30* encodes a member of claudin superfamily of four-transmembrane domain proteins (Smith et al., 2013). The striking similarity of the *hpo-30* and *dma-1* branching defects is indicative of shared function; in both cases, truncated 2^0 branches emerge during early larval development but 3^0 and 4^0 dendrites are rarely produced (O. W. Liu and Shen, 2011; Smith et al., 2013). Live cell imaging in PVD with fluorescently-tagged HPO-30 and DMA-1 detected co-localization and strong FRET (fluorescence resonance energy transfer) that is indicative of their close proximity *in vivo* (Zou et al., 2018). In addition, a co-immunoprecipitation experiment confirmed that HPO-30 binds DMA-1 and that the DMA-1 ICD is not required for this interaction (Fig. 2B) (L. T. Tang et al., 2019). Thus, DMA-1 binds TIAM-1 via the DMA-1 C-terminal PDZ motif and HPO-30 through either the DMA-1 transmembrane or extracellular domains. Additional findings suggested that these separate interactions of DMA-1 with TIAM-1 and HPO-30 are both required for PVD branching. For example, the HPO-30 C-terminus recruits the WAVE regulatory complex (WRC) (Zou et al., 2018). The WRC is known to activate the Arp2/3 complex which in turn promotes assembly of branched actin filaments (Takenawa and Suetsugu, 2007). PVD branching is strongly impaired by mutations that disable GEX-3, the *C. elegans* homolog of the WRC component, Nap1 (Zou et al., 2018), thus suggesting that HPO-30 complexes with the WRC to regulate actin assembly for dendrite outgrowth (Fig. 2A). Transgenic expression of DMA-1Δ4AA restores 2^0 and 3^0 branches to a *dma-1* null allele but not 4^0 dendrites thereby indicating that TIAM-1 is required for 4^0 branches but that DMA-1Δ4AA, potentially through interactions with HPO-30, is sufficient for 2^0 and 3^0 branching. This idea is substantiated by the observation that the DMA-1Δ4AA branching defect is worsened by an HPO-30 mutant protein with a C-terminal mutation that blocks WRC binding. Together, these results suggest a model in which DMA-1 and HPO-30 act in tandem to recruit specific regulators of actin assembly (TIAM-1 and WRC) that then function in close proximity to drive dendritic branching (Zou et al., 2018).

An obvious model is suggested by these findings: The GEF activity of TIAM-1 could activate a Rac GTPase which then stimulates the nearby WRC to trigger actin assembly (Takenawa and Suetsugu, 2007). This straightforward idea is confounded, however, by two additional observations. First, a point mutation that specifically disables TIAM-1 GEF activity does not disrupt PVD branching. Second, neither the small GTPases, MIG-2/RhoG and CED-10/Rac1 that are known to function downstream of TIAM-1 in axon guidance (Demarco et al., 2012), nor RAC-2 are required for PVD dendrite morphogenesis (L. T. Tang et al., 2019). Biochemical experiments confirm that TIAM-1 binds ACT-4, however, and thus suggest that TIAM-1 links the DMA-1 receptor complex to actin via a non-canonical mechanism (L. T. Tang et al., 2019). Whether this interaction actually stimulates actin assembly has not been directly established nor the mechanism whereby DMA-1 interaction with its ligands SAX-7, MNR-1 and LECT-2 activates this pathway.

10. The unfolded protein response (UPR) pathway is normally activated in the endoplasmic reticulum (ER) to deliver DMA-1 to branching dendrites

Forward genetic screens detected mutations in *ire-1*, a key regulator of the unfolded protein response (UPR) that disrupt PVD branching (Salzberg et al., 2017; Wei et al., 2015). Ire1 (Inositol-Requiring Enzyme 1) functions as a sentinel in the ER to detect unfolded proteins and trigger the UPR for ER protein homeostasis. IRE1 regulates multiple downstream effectors including (1) the transcription factor, XBP-1, that regulates expression of chaperones as well as ERAD-associated proteins that drive proteolysis and (2) the RIDD (Regulated Ire1-Dependent Decay) pathway that cleaves mRNAs for specific ER proteins (Maurel et al., 2014). Although XBP-1 is upregulated in PVD, with peak activity occurring as dendrites are actively branching during development, a loss-of-function *xbp-1* mutant has no visible effect on PVD morphology (Salzberg et al., 2017; Wei et al., 2015). Genetic disruption of the RIDD pathway, however, does result in a weak PVD branching defect which is likely indicative of a complex downstream mechanism involving multiple UPR pathways (Wei et al., 2015). Interestingly, activation of the UPR in PVD depends on DMA-1. Moreover, trafficking of DMA-1 from the ER to the dendrite membrane requires *ire-1* function. Together, these results suggest that the UPR is normally activated in PVD to insure that DMA-1, a highly expressed ER protein that is necessary for branching, is efficiently delivered to growing dendrites. This pathway is also active in the FLP neuron but is not required in other *C. elegans* neurons with a less-elaborate dendrite morphology (Salzberg et al., 2017; Wei et al., 2015). This role is likely conserved because *ire1* knock down in mammalian hippocampal neurons also limits dendrite growth (Saito et al., 2018; Salzberg et al., 2017). Finally, a recent study showed that ER tubules normally invade PVD 2^0 branches and that atlastin, a dynamin-like GTPase and key regulator of ER morphogenesis, is required for *ire1*-dependent PVD branching (X. Liu et al., 2019).

11. Self-avoidance sculps PVD dendrite morphology

Thus far, we have described mechanisms that promote dendrite growth. The final architecture of the PVD arbor also requires separate mechanisms that have the opposite effect of restraining dendrite elongation. This possibility was first detected by time-lapse imaging of PVD morphogenesis during larval development. PVD lateral dendrites emerge via a series of orthogonal branching events. Notably, each 2^0 branch typically gives rise to a pair of sublateral 3^0 dendrites that point in opposite directions along the body axis. Although this configuration results in 3^0 branches from adjacent menorahs growing toward one another, they rarely overlap. Opposing 3^0 branches eventually contact one another but then retract, in some cases after several successive contact events (Smith et al., 2010, 2012) (Fig. 4A). This phenomenon of self-avoidance has been widely observed and may be a universal feature

of neurons (Grueber and Sagasti, 2010; Kramer and Stent, 1985). As might be expected for a mechanism that involves direct contact, cell surface proteins such as Dscam and protocadherin are known to mediate dendrite self-avoidance (Fuerst et al., 2009; Lefebvre et al., 2012; Matthews et al., 2007). Surprisingly, a soluble ligand, UNC-6/Netrin, also mediates PVD dendrite self-avoidance in concert with its cognate receptors, UNC-40/DCC and UNC-5 (Smith et al., 2010; Sundararajan et al., 2018) (Fig. 4A). In *C. elegans* larvae, UNC-6/Netrin is secreted from specific ventrally-located motor neurons and epidermal cells to guide circumferential axon outgrowth by functioning either as an attractant that interacts with UNC-40/DCC or as a repellent via UNC-5 or UNC-5/UNC-40 heterodimeric receptors (Norris et al., 2014; Wadsworth et al., 1996). Because the ventral source for UNC-6/Netrin is necessary for the fidelity of these axon guidance choices, a graded UNC-6/Netrin signal has been proposed to drive dorsal vs ventral axonal trajectories (Wadsworth, 2002). For PVD self-avoidance, however, UNC-6/Netrin, like LECT-2, appears to function as a permissive cue (Díaz-Balzac et al., 2016; Smith et al., 2012; Zou et al., 2016). Ectopic expression of UNC-6/Netrin from other cell types including PVD or global expression from a heat-shock promoter, for example, was sufficient to rescue the PVD self-avoidance defect of *unc-6* mutants. Rescue experiments also demonstrated that UNC-40/DCC and UNC-5 must be expressed in PVD for self-avoidance (Smith et al., 2012). Because earlier work showed that UNC-6/Netrin could be captured by Frazzled, the *Drosophila* UNC-40/DCC homolog, on guidepost cells to steer nearby migrating axon growth cones (Hiramoto et al., 2000), it was proposed that UNC-40/DCC similarly captures UNC-6/Netrin at the tips of PVD 3^0 dendrites and that this configuration then triggers mutual retraction upon contact with UNC-5 on an opposing 3^0 dendrite. This model predicts that UNC-6/Netrin can function as a short-range cue which was demonstrated by an experiment in which expression in PVD of a chimeric protein composed of UNC-6 fused to the extracellular domain of UNC-40 was sufficient to restore self-avoidance to an *unc-6* mutant. Additional genetic results suggest, however, that UNC-40/DCC may also function in a parallel-acting self-avoidance pathway that does not require UNC-6/Netrin (Smith et al., 2012). A role for UNC-40 in PVD dendrite repulsion has also been observed for the interesting case in which a genetic mutation in the *lin-22* locus results in the production of multiple adjacent PVD-like neurons which occupy discrete domains or "tile" and do not invade each other's territories due to *unc-40* function (Yip and Heiman, 2016).

12. Actin polymerization and non-muscle myosin activity drive UNC-6-dependent dendrite self-avoidance

As noted above, the actin cytoskeleton is necessary for expansion of the PVD dendritic arbor (L. T. Tang et al., 2019; Zou et al., 2018). Surprisingly, recent results indicate that actin assembly is also required for dendrite retraction in the self-avoidance response (Liao et al., 2018; Sundararajan et al., 2018). Mutations that disable TIAM/GEF or the WRC, both positive regulators of actin polymerization, block outgrowth of higher order PVD dendrites (L. T. Tang et al., 2019; Zou et al., 2018). In contrast, genetic mutants of an alternative set of protein components that also promote F-actin elongation do not prevent outgrowth of PVD lateral dendrites but do impair dendrite shortening during self-avoidance (Liao et al., 2018; Sundararajan et al., 2018). For example, Ena/VASP prevents actin capping proteins from binding to the plus-end of F-actin thereby facilitating F-actin growth. A mutation that disables UNC-34, the *C. elegans* homolog of Ena/VASP, impairs self-avoidance but not outgrowth (Sundararajan et al., 2018). Genetic mutants of other regulators of actin polymerization including MIG-10/Lamellipodin, UNC-73/GEF, WSP-1/WASP and RNAi knockdown of the Arp2/3 complex also disrupt dendrite retraction but not overall growth (Fig. 4B) (Liao et al., 2018; Sundararajan et al., 2018). Additional experiments indicate that UNC-6/Netrin signaling triggers actin polymerization via these components for self-avoidance. For example, a mutation that disables WSP-1/WASP does not enhance the PVD self-avoidance defect of *unc-6/Netrin* mutants which suggests that WSP-1/WASP and UNC-6/Netrin function in a common pathway. Similarly, a myristoylated version of UNC-5 that lacks its extracellular UNC-6/Netrin binding domain is constitutively active (Norris et al., 2014) (Norris et al., 2014) and can rescue the Unc-6 self-avoidance defect but does not restore dendrite retraction to an *unc-34/Ena/VASP* mutant. This finding suggests that the UNC-6/Netrin receptor, UNC-5, functions upstream of UNC-34/Ena/VASP to drive self-avoidance. A downstream role for UNC-34/Ena/VASP in UNC-6/Netrin-mediated self-avoidance is consistent with previous results showing that UNC-34/Ena/VASP is required for UNC-5 and UNC-6/Netrin to induce axon repulsion (Colavita and Culotti, 1998; Sundararajan et al., 2018).

The paradoxical idea that F-actin growth can result in dendrite shortening is explained by the finding that non-muscle myosin is necessary for UNC-6/Netrin-mediated self-avoidance. A mutation in NMY-1, a member of the myosin II family, results in a self-avoidance defect that is rescued by PVD expression of wild-type NMY-1 (Sundararajan et al., 2018). This finding suggests that NMY-1/myosin functions in PVD to engage a nascent actin cytoskeleton for dendrite retraction in mechanism that could involve the acceleration of retrograde flow (Mitchison and Cramer, 1996). This model is supported by the additional finding that a phosphomimetic mutant of the myosin regulatory light chain, MLC-4, that constitutively activates NMY-1/myosin function (K. Ono and S. Ono, 2016), also rescues the Unc-6/Netrin PVD self-avoidance defect (Sundararajan et al., 2018). In some respects, these findings parallel earlier results from studies in diverse species suggesting that both actin polymerization and non-muscle myosin can mediate axonal growth cone retraction induced by netrin, slit or semaphoring (Bashaw et al., 2000; Brown and Bridgman, 2009; Brown et al., 2009; Chang et al., 2006; Gallo, 2006; McConnell et al., 2016; Murray et al., 2010). In addition, recent results indicate that both slit and semaphorin can drive dendrite self-avoidance (Gibson et al., 2014; Matsuoka et al., 2012). Thus, similar actomyosin-dependent mechanisms may be employed in both dendrites and axons to mediate filopodial retraction in response to repulsive cues.

A recent report described an additional PVD self-avoidance mechanism involving the membrane protein MIG-14/Wntless (Liao et al., 2018). Although MIG-14 and other homologs (Wntless in *Drosophila* and G-protein coupled receptor 177 in humans) are required for Wnt secretion (Port and Basler, 2010), Wnt function is not necessary for MIG-14/Wntless-dependent self-avoidance in PVD. This effect could be due to homotypic interactions because ectopic expression of MIG-14/Wntless in bundled touch neuron branches is sufficient to induce de-fasciculation. RNAi knockdown of Wntless in *Drosophila* also results in dendrite self-avoidance defects which suggests that this novel mechanism is conserved. Genetic data indicate that MIG-14/Wntless functions in parallel to UNC-40/DCC for PVD self-avoidance but also likely depends on nascent actin polymerization for dendrite retraction (Liao et al., 2018). Notably, this work shows that self-avoidance is defective in a mutant of *wve-1*/WAVE, which suggests that the WRC could function in both outgrowth and retraction. Additional genetic results reported in this work indicate that WSP-1/WASP acts downstream of MIG-14/Wntless (Liao et al., 2018). This result, however, conflicts with the independent finding that WSP-1/WASP functions in the UNC-6/Netrin self-avoidance mechanism (Sundararajan et al., 2018).

13. Balancing actin polymerization for growth vs retraction determines dendrite length

Strikingly, as noted above, distinct sets of actin regulatory proteins are involved in PVD dendrite outgrowth mediated by the DMA-1 receptor complex (TIAM-1/GEF and WRC) (L. T. Tang et al., 2019; Zou et al., 2018) vs retraction that depends on UNC-6/Netrin signaling (UNC-34/Ena/VASP, UNC-73/GEF, MIG-10/Lpd, WSP-1/WASP and the Arp2/3 complex) (Liao et al., 2018; Sundararajan et al., 2018) (Fig. 4C). Dysregulation of either pathway can alter net dendrite length. For

example, adjacent 3^0 dendrites over-grow one another in *unc-34/Ena/-VASP* mutants but are foreshortened when TIAM/GEF is disabled (Smith et al., 2012; Sundararajan et al., 2018; L. T. Tang et al., 2019; Zou et al., 2018). Additional genetic results suggest that these opposing pathways are balanced in the wild type to specify dendrite length. Hyperactivation of the DMA-1 pathway either by transgenic over-expression of DMA-1 or in *kpc-1* mutants induces a strong self-avoidance defect (Dong et al., 2016; O. W. Liu and Shen, 2011; Salzberg et al., 2014). In the *kpc-1(xr58)* hypomorphic mutant, for example, about half of 3^0 dendrites fail to self-avoid and this defect is suppressed by a *dma-1* loss-of-function mutant. The interpretation of this finding is that KPC-1 normally functions to temporally down-regulate DMA-1 surface expression in 3^0 dendrites and hence weaken interactions with the sublateral SAX-7 epidermal stripes to facilitate the orthogonal turn of the 3^0 dendrites onto the narrow circumferential SAX-7 bands adjacent to body muscles (Fig. 3B) (Dong et al., 2016; O. W. Liu and Shen, 2011). This model predicts that UNC-6/Netrin-driven self-avoidance should oppose DMA-1-dependent dendrite outgrowth (Fig. 4C). A genetic test is consistent with this idea. Both *kpc-1* and *unc-6* mutants are recessive; the heterozygous *kpc-1/+* and *unc-6/+* strains show normal PVD lateral branch outgrowth and self-avoidance responses. Thus, a 50% reduction in either *kpc-1* or *unc-6* gene function does not perturb dendrite morphogenesis. The simultaneous halving of gene dosage for both loci in a *kpc-1/+; unc-6/+* double heterozygote, however, results in ~30% of adjacent 3^0 dendrites failing to self-avoid. This effect depends on DMA-1 because a concomitant 50% reduction of *dma-1* function fully suppresses the *kpc-1/+; unc-6/+* self-avoidance defect (Sundararajan et al., 2018). Thus, the net length of each 3^0 dendrite is determined by the opposing effects of the UNC-6/Netrin pathway vs the DMA-1 receptor complex. A crucial role for the actin cytoskeleton in the determination of dendrite length is consistent with the observation that actin is enriched in elongating PVD branches and thus available for regulation by both pathways (Liao et al., 2018; Sundararajan et al., 2018; L. T. Tang et al., 2019; Zou et al., 2018). The physical disposition of each separate set of actin regulators for growth vs retraction and the cytoskeletal structures that they control, however, have not been resolved. Indeed, this task is complicated by rapid fluctuations in the F-actin signal near the tips of growing PVD dendrites (Liao et al., 2018; Sundararajan et al., 2018). This dynamic behavior resembles that of the recently described “actin blobs” in highly branched da IV sensory neurons in *Drosophila* and thus may be indicative of a conserved role for the actin cytoskeleton in dendrite length determination (Nithianandam and Chien, 2018; Sundararajan et al., 2018). An over-arching challenge for the future is to elucidate the downstream mechanism that integrates the opposing pathways for driving actin polymerization for dendrite growth vs retraction (Fig. 4C).

14. Dendrite regeneration and self-avoidance

Mechanisms that drive axon regeneration have been extensively investigated but much less is known of the molecular pathways that repair injured dendrites (Bejjani and Hammarlund, 2012). Recent studies have exploited the highly branched PVD dendritic arbor to investigate this question (Kravtsov et al., 2017; Oren-Suissa et al., 2017). Laser ablation of the PVD 1^0 dendrite (“dendrotomy”) at the L4 stage evokes a series of morphological responses. First, the severed ends of ~40% of 1^0 dendrites elongate until reannealing at the site of injury. Remarkably, 3^0 branch outgrowth is also stimulated leading to extensive self-avoidance defects and eventual fusion of adjacent menorahs that depends on the fusion-promoting membrane protein, AFF-1. Additional responses to the injury include ectopic sprouting as well as pruning by the AFF-1 paralog, EFF-1. These results suggest that dendrotomy evokes a global PVD response to injury that promotes dendrite growth and self-fusion thereby effectively disabling the self-avoidance response (Oren-Suissa et al., 2017). In *C. elegans*, axonal injury triggers a rise in intracellular Ca^{++} that promotes regeneration (Ghosh-Roy et al., 2010; Sun et al., 2014). Whether this effect is also involved in the PVD response to dendritic injury has not been determined. Indeed, genetic mutations that result in reduced levels of intracellular Ca^{++} are correlated with extensive self-avoidance defects (Cohen et al., 2014) which points to the alternative possibilities that Ca^{++} is either reduced by dendritic injury or that both regeneration and self-avoidance depend on homeostatic maintenance of Ca^{++} concentration within a medial range. A subsequent study uncovered additional links between dendrite regeneration and self-avoidance. The regenerative capacity of PVD dendrites declines with age and this negative effect depends in part on the DAF-2/DAF-16 insulin/IGF1 signaling pathway as also observed for axons (Byrne et al., 2014; Kravtsov et al., 2017). The DAF-2/DAF-16 pathway also promotes self-avoidance (Kravtsov et al., 2017). Although the downstream mechanism of this effect is unknown, it will be interesting to determine if it depends on the recently discovered role of DAF-16 in an alternative UPR-like pathway that directs DMA-1 trafficking from the ER to the dendrite surface (Salzberg et al., 2017).

15. Microtubules in PVD dendrite morphogenesis

Microtubules are predominantly located in the PVD axon and 1^0 dendrites (Maniar et al., 2011; Sundararajan et al., 2018). Experiments with the plus-end marker, EB2:GFP, revealed a surprising feature of PVD microtubule organization. As commonly observed across species, microtubules in the PVD axon are oriented plus-end out (e.g., toward the axon tip). In contrast, dendrites typically show a microtubule minus-end out orientation and this feature is also observed for the PVD anteriorly-directed 1^0 dendrite. The posterior PVD 1^0 dendrite, however, shows a microtubule plus-end out orientation resembling that of the PVD axon (Fig. 5). Thus, microtubules in PVD 1^0 dendrites are oriented in a single direction along the body axis with minus-ends pointing anteriorly and plus ends directed toward the posterior (Taylor et al., 2015).

PVD branching is altered by mutations in microtubule-dependent motors. Mutants that disrupt the minus-end directed dynein complex, for example, result in fewer branches toward the tip of the anterior 1^0 PVD dendrite (Aguirre-Chen et al., 2011; Taylor et al., 2015). This phenotype is consistent with the idea that dynein activity directs branching factors along a microtubule track toward the distal region (minus-end) of the anterior PVD 1^0 dendrite. Mutations that disable the plus-end directed motor, UNC-116/Kinesin-1, also disrupt PVD branching. Surprisingly, the PVD branching defect of *unc-116* mutants strongly resembles that of dynein-defective mutants (e.g., reduced anterior branching). The likely explanation for this outcome is that *unc-116* activity is required for maintaining the minus-end out orientation of the anterior 1^0 PVD dendrite, an UNC-116/Kinesin-1 function that is also observed in other *C. elegans* neurons (Yan et al., 2013). In an *unc-116* mutant, the anterior 1^0 dendrite adopts a plus-end out orientation such that dynein activity, in this case, should promote trafficking toward the cell soma thus resulting in distal anterior branching defects resembling that of a dynein mutant (Taylor et al., 2015). These results suggest that the dual roles of dynein and UNC-116/kinesin are required for PVD dendrite branching.

Mutations that disable RAB-10/GTPase provide additional clues to the role of microtubule structure in PVD dendritic branching; in *rab-10* mutants, branches are dramatically reduced in regions proximal to the PVD soma and conversely increased, relative to wild type, at the distal end of the anterior 1^0 dendrite (Taylor et al., 2015; Zou et al., 2015). RAB-10 is highly conserved and functions in multiple endocytic and exocytic pathways including interactions with kinesin-1 motor complexes to mediate plus-end-directed vesicular transport (Chua and B. L. Tang, 2018). Thus, in this case, increased branching complexity at the distal anterior PVD region could result from disrupted plus-end directed transport of branch promoting factors toward the cell soma by UNC-116/Kinesin-1. Genetic experiments are consistent with this interpretation (Taylor et al., 2015). In addition to mediating vesicular trafficking, RAB-10 is also known to interact with the exocyst complex to target post-golgi vesicles for fusion with the plasma membrane (Chua and

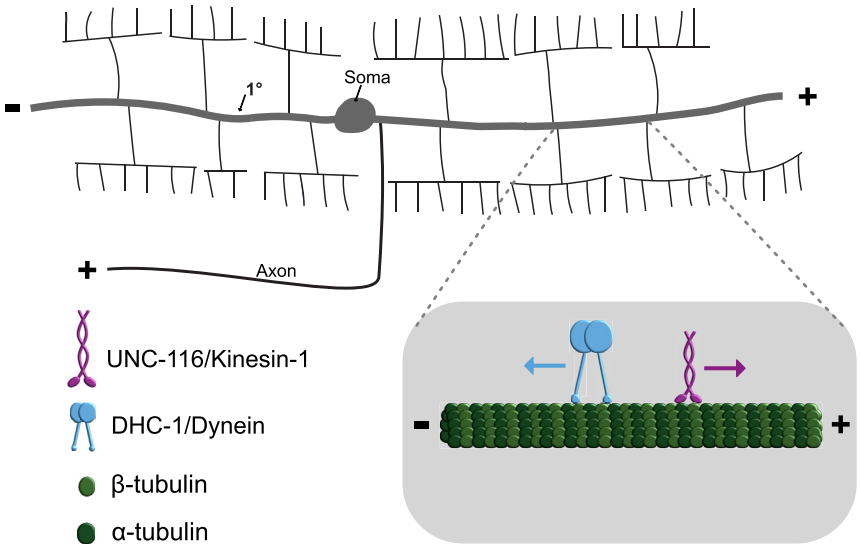

Fig. 5. Microtubule orientation and motors in PVD dendrites. Microtubule (MT) orientation in PVD 1^0 dendrite with anterior minus-end (-) and posterior plus-end (+). MTs are oriented plus-end (+) out in the axon. Inset shows directionality of the plus-end microtubule motor, UNC-116/Kinesin-1, and minus-end motor, DHC-1/Dynein in the 1^0 dendrite.

B. L. Tang, 2018). This additional role for RAB-10 in dendrite branching is suggested by the finding that exocyst complex mutations phenocopy the loss of posterior branches in *rab-10* mutants (Taylor et al., 2015). Genetic manipulations that fully disable exocyst function in PVD almost completely block branching which points to additional roles for the exocyst complex in dendritic morphogenesis that do not require RAB-10 (Zou et al., 2015). Branching defects for mutations that disable microtubule-dependent motors and vesicular trafficking are linked to disrupted delivery of the branch promoting factors, DMA-1 and HPO-30 (Taylor et al., 2015; Zou et al., 2015). Both DMA-1 and HPO-30 fail to localize to dendritic membranes but are sequestered in intracellular vesicles in PVD dendrites in *rab-10* and exocyst mutants thus suggesting that post-Golgi vesicular trafficking of DMA-1 and HPO-30 to the plasma membrane is required for stabilizing PVD dendritic branches (Zou et al., 2015). Recent studies indicate that microtubules are present in lateral PVD dendrites and thus could function in these structures for trafficking of DMA-1 and HPO-30 and other branching factors (Harterink et al., 2018; Richardson et al., 2014). These findings are significant because all of these components are conserved and thus likely to exert similar functions in mammalian neurons.

16. Transcriptional control of dendrite morphogenesis

The stereotypical development of the PVD dendritic arbor throughout most of larval development could reflect the step-wise execution of a transcriptionally regulated developmental program. The POU domain transcription factor, UNC-86 and its target, the LIM homeodomain protein, MEC-3 are both necessary for the PVD harsh touch response (Way and Chalfie, 1989) and likely function sequentially with UNC-86 required for the generation of the nascent PVD neuron and MEC-3 for subsequent higher order dendritic branching (Smith et al., 2013, 2010; Tsalik et al., 2003). A microarray profile of PVD and OLL neurons confirmed enriched expression of *unc-86* and *mec-3* along with ~100 additional transcription factors. An RNAi screen detected PVD defects in ~10% of the transcription factor genes in this data set (Smith et al., 2010). Notable hits included the HOX family homeodomain protein, LIN-39, which is required for the emergence of the PVD soma and the Zn finger/Nerfin homolog EGL-46 that specifies a subset of PVD 2° branches (see below). Although initial RNAi results suggested that AHR-1 (aryl hydrocarbon receptor/spineless) functioned to limit PVD 2° branching, a more careful analysis revealed that the apparently increased number of 2° branches in an *ahr-1* mutant was due to the transformation of AVM, an anteriorly located touch neuron, into an additional PVD-like cell that adopts both the highly branched architecture and function of PVD (Fig. 6A–C). Analysis of the ZFH class transcription factor, ZAG-1, revealed a similar phenotype for a *zag-1* mutant in which the posterior touch neuron, PVM, adopts a PVD-like fate (Smith et al., 2013, 2010). Thus, the transcription factors AHR-1 and ZAG-1 are expressed in subsets of touch neurons (i.e., AVM and PVM, respectively) to block the activation of a default genetic program for the PVD fate. Detailed analysis of the *ahr-1* mutant phenotype determined that (1) AHR-1 normally elevates *mec-3* expression in AVM while (2) simultaneously antagonizing MEC-3 targets that promote lateral branching. This model provides a mechanistic explanation for how *mec-3* can specify both touch neuron and PVD differentiation; low levels of MEC-3 are sufficient to activate PVD-specific genes but these genes are not turned on in touch neurons that express high levels of MEC-3 because AHR-1 selectively blocks these targets. A microarray profiling experiment was performed to identify potential *mec-3*-regulated genes that could be used to test this model. This approach determined that *mec-3* promotes expression of the claudin-like protein HPO-30 in PVD for lateral branching and that *ahr-1* negatively regulates *hpo-30* in touch neurons to prevent the elaboration of a PVD-like dendritic arbor (Smith et al., 2013). The finding that the *Drosophila* AHR-1 homolog, Spineless, also regulates sensory neuron branching (Kim et al., 2006) suggests that this function is evolutionarily conserved and thus that mammalian members of the aryl hydrocarbon receptor class of transcription factors may perform a similar function. Regulatory mechanisms that link distinct levels of transcription factor expression to specific dendrite morphologies (viz, MEC-3), may also represent an evolutionarily conserved strategy for diversifying dendritic architecture. The branching complexity of different classes of larval sensory neurons in Drosophila, for example, is directly related to expression of the transcription factor, Cut, which in turn functions in a genetic cascade to control downstream transcription factor effectors of dendrite growth (Corty et al., 2016; Grueber et al., 2003).

17. Separate transcriptionally regulated pathways for distinct classes of lateral PVD dendrites

Although PVD lateral branching is substantially diminished in *hpo-30* mutants, some 2° branches are still produced with the majority located on the right side of the animal (i.e. PVDR). Notably, these residual 2° branches are fasciculated with motor neuron commissures which are predominantly located on the right (White et al., 1986). This finding is

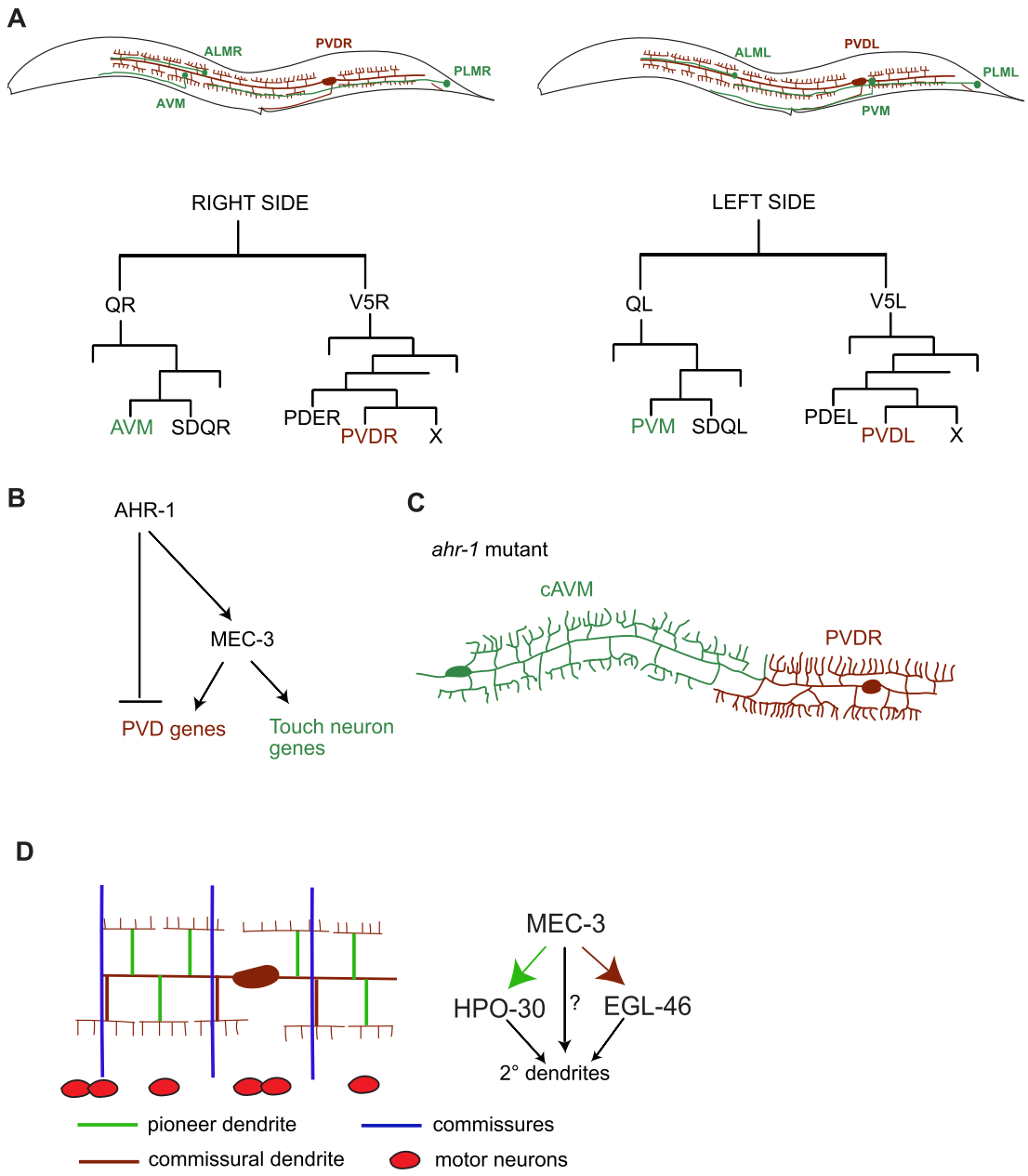

Fig. 6. Transcriptional regulation of PVD morphogenesis (A) Schematics of mechanosensory neurons on the right and left sides of the worm and corresponding with the cell lineages. Unbranched touch neurons are AVM, ALMR and PLMR on the right and PVM, ALML and PLML on the left. Note PVDR on the right and PVDL on the left. (B) A model for AHR-1-dependent transcriptional regulation of PVD and touch neuron fate (C) Tracings of a converted AVM (cAVM) and PVD neuron in an *ahr-1* mutant background. (D) Schematic of pioneer PVD 2^0 dendrites (green) that grow on the inside surface of the epidermis vs commissural 2^0 dendrites that also fasciculate with motor neuron commissures (red). The MEC-3 transcription factor promotes expression of the transcription factor EGL-46/TFIIA Zinc finger and HPO-30/Claudin. EGL-46 is required for outgrowth of 2^0 dendrites that fasciculate with motor neuron commissures and HPO-30/Claudin mediates extension of pioneer 2^0 dendrites. MEC-3 also regulates expression of additional branching factors (?).

consistent with the idea that HPO-30 is preferentially required for stabilizing "pioneer" vs "commissural" 2° branches that grow out along motor neuron commissures (Fig. 6D). Neither type of 2° branch is produced in *mec-3* mutants which suggests that an additional *mec-3* target could be selectively required for the outgrowth of commissural 2° branches to function in parallel to HPO-30 (Smith et al., 2013). The Zn finger/Nerfin transcription factor, EGL-46, was a strong candidate for this role because *egl-46* mutants show a preferential reduction of 2° branches in PVDR vs PVDL (O'Brien et al., 2017). Direct inspection showed that commissural branches are selectively reduced in *egl-46* mutants. That EGL-46 functions as a transcription factor in PVD to promote commissural branching is consistent with a rescue experiment showing that EGL-46 is cell autonomous for PVD and the finding that its canonical heteromeric partner, the TEAD domain transcription factor EGL-44 is also preferentially required for commissural branching. Finally, the mutant effects of *hpo-30* and *egl-44* are additive as indicated by an overall reduction in both pioneer and commissural branches when both pathways are genetically disabled. However, additional MEC-3-regulated targets are also likely required because about half of all PVD 2° branches remain in *egl-44;hpo-30* double mutants but are completely absent in *mec-3* animals. Moreover, additional genetic experiments indicated that EGL-46 could also function in parallel to MEC-3 to regulate a subset of PVD-specific genes (O'Brien et al., 2017).

18. Conclusions and future prospects

The PVD nociceptor has served as a highly useful experimental system for investigating the genetic and cell biological pathways that drive dendritic branching. Ready access of PVD to live cell imaging and the utility of mutant analysis largely accounts for the rapid progress over the past few years. Notable achievements include the discovery of a multi-component receptor complex (i.e., DMA-1, HPO-30, LECT-2, SAX-7, MNR-1) that patterns dendritic branching and its interactions with actin-binding proteins that may drive dendrite elongation on the epidermis (L. T. Tang et al., 2019; Zou et al., 2018). The finding that dendrite retraction in the self-avoidance response depends on different regulators of actin dynamics poses the challenging question of how these opposing pathways for growth vs retraction are coordinated to define dendrite length. Dendrite growth critically depends on DMA-1 and at least two regulatory mechanisms involving KPC-1 and the unfolded protein response (UPR) that modulate DMA-1 trafficking and surface expression (Wei et al., 2015). An interesting question is whether these pathways are regulated during outgrowth by either an intrinsic program or by feedback signals generated at each step of dendrite growth. For example, does contact between sister 3^0 dendrites and the consequent activation of UNC-6/Netrin (Smith et al., 2012; Sundararajan et al., 2018) and MIG-14/Wntless-mediated dendrite retraction (Liao et al., 2018) also reduce DMA-1 surface expression by activating KPC-1? Although the DMA-/HPO-30 receptor complex is a principle driver of PVD dendrite morphogenesis, additional factors for interaction with motor neuron commissures are likely also required to achieve the full wild-type complement of menorahs. Pathways for initiating PVD branching are similarly unknown. In addition to lacking all lateral branches, PVD 1° dendrites in *mec-3* mutants also fail to initiate the saltatory extension and retraction of lateral filopodia that normally precede 2^0 branch outgrowth (Smith et al., 2010). The fact that extensive forward genetic screens have not detected mutants that exactly phenocopy *mec-3*, suggests that more than one *mec-3*-regulated target could be required. The use of new methods for generating cell specific RNA-Seq profiles (Spencer et al., 2014) could be used to identify MEC-3 regulated targets in PVD for reverse genetic screens to address this question. Finally, a subject that this review has not addressed, the relationship of the PVD dendrite arbor to its nociceptive function is an important, and largely unexplored question (Chen et al., 2019; Husson et al., 2012).

Acknowledgements

We thank Hannes Bulow and Chun-Liang Pan for sharing unpublished findings. This work was supported by NIH Grant R01 NS079611 to DMM and a Vanderbilt Academic Pathways Fellowship to JS.

References

Abraira, V.E., Kuehn, E.D., Chirila, A.M., Springel, M.W., Toliver, A.A., Zimmerman, A.L., Orefice, L.L., Boyle, K.A., Bai, L., Song, B.J., Bashista, K.A., O'Neill, T.G., Zhuo, J., Tsan, C., Hoynoski, J., Rutlin, M., Kus, L., Niederkofler, V., Watanabe, M., Dymecki, S.M., Nelson, S.B., Heintz, N., Hughes, D.I., Ginty, D.D., 2017. The cellular and synaptic architecture of the mechanosensory dorsal horn. Cell 168, 295–310. https://doi.org/10.1016/j.cell.2016.12.010 e19.

Aguirre-Chen, C., Bulow, H.E., Kaprielian, Z., 2011. C. elegans bicd-1, homolog of the Drosophila dynein accessory factor Bicaudal D, regulates the branching of PVD sensory neuron dendrites. Development 138, 507–518. https://doi.org/10.1242/dev.060939.

Albeg, A., Smith, C.J., Chatzigeorgiou, M., Feitelson, D.G., Hall, D.H., Schafer, W.R., Miller III, D.M., Treinin, M., 2011. C. elegans multi-dendritic sensory neurons: morphology and function. Mol. Cell. Neurosci. 46, 308–317. https://doi.org/10.1016/j.mcn.2010.10.001.

Bashaw, G.J., Kidd, T., Murray, D., Pawson, T., Goodman, C.S., 2000. Repulsive axon guidance: abelson and Enabled play opposing roles downstream of the roundabout receptor. Cell 101, 703–715.

Bejjani, R.E., Hammarlund, M., 2012. Neural regeneration in Caenorhabditis elegans. Annu. Rev. Genet. 46, 499–513. https://doi.org/10.1146/annurev-genet-110711-155550.

Brown, J.A., Bridgman, P.C., 2009. Disruption of the cytoskeleton during Semaphorin 3A induced growth cone collapse correlates with differences in actin organization and associated binding proteins. Dev. Neurobiol. 69, 633–646. https://doi.org/10.1002/dneu.20732.

Brown, J.A., Wysolmerski, R.B., Bridgman, P.C., 2009. Dorsal root ganglion neurons react to semaphorin 3A application through a biphasic response that requires multiple myosin II isoforms. Mol. Biol. Cell 20, 1167–1179. https://doi.org/10.1091/mbc.E08-01-0065.

Byrne, A.B., Walradt, T., Gardner, K.E., Hubbert, A., Reinke, V., Hammarlund, M., 2014. Insulin/IGF1 signaling inhibits age-dependent axon regeneration. Neuron 1–13. https://doi.org/10.1016/j.neuron.2013.11.019.

Celestrin, K., Díaz-Balzac, C.A., Tang, L.T.H., Ackley, B.D., Bülow, H.E., 2018. Four specific immunoglobulin domains in UNC-52/Perlecan function with NID-1/Nidogen during dendrite morphogenesis in Caenorhabditis elegans. Development 145, dev158881. https://doi.org/10.1242/dev.158881.

Chang, C., Adler, C.E., Krause, M., Clark, S.G., Gertler, F.B., Tessier-Lavigne, M., Bargmann, C.I., 2006. MIG-10/lamellipodin and AGE-1/PI3K promote axon guidance and outgrowth in response to slit and netrin. Curr. Biol. 16, 854–862. https://doi.org/10.1016/j.cub.2006.03.083.

Chatzigeorgiou, M., Yoo, S., Watson, J.D., Lee, W.-H., Spencer, W.C., Kindt, K.S., Hwang, S.W., Miller III, D.M., Treinin, M., Driscoll, M., Schafer, W.R., 2010. Specific roles for DEG/ENaC and TRP channels in touch and thermosensation in C. elegans nociceptors. Nat. Neurosci. 13, 861–868. https://doi.org/10.1038/nn.2581.

Chen, L., Zhou, S., 2010. "CRASH"ing with the worm: insights into L1CAM functions and mechanisms. Dev. Dyn. 239, 1490–1501. https://doi.org/10.1002/dvdy.22269.

Chen, C.-H., Hsu, H.-W., Chang, Y.-H., Pan, C.-L., 2019. Adhesive L1CAM-robo signaling aligns growth cone F-actin dynamics to promote axon-dendrite fasciculation in C. elegans. Dev. Cell 48, 215–228. https://doi.org/10.1016/j.devcel.2018.10.028 e5.

Chua, C.E.L., Tang, B.L., 2018. Rab 10-a traffic controller in multiple cellular pathways and locations. J. Cell. Physiol. 233, 6483–6494. https://doi.org/10.1002/jcp.26503.

Cohen, E., Chatzigeorgiou, M., Husson, S.J., Steuer-Costa, W., Gottschalk, A., Schafer, W.R., Treinin, M., 2014. Caenorhabditis elegans nicotinic acetylcholine receptors are required for nociception. Mol. Cell. Neurosci. 59, 85–96. https://doi.org/10.106/j.mcn.2014.02.001.

Colavita, A., Culotti, J.G., 1998. Suppressors of ectopic UNC-5 growth cone steering identify eight genes involved in axon guidance in Caenorhabditis elegans. Dev. Biol. 194, 72–85. https://doi.org/10.1006/dbio.1997.8790.

Corty, M.M., Tam, J., Grueber, W.B., 2016. Dendritic diversification through transcription factor-mediated suppression of alternative morphologies. Development 143, 1351–1362. https://doi.org/10.1242/dev.130906.

Delandre, C., Amikura, R., Moore, A.W., 2016. Microtubule nucleation and organization in dendrites. cc 15, 1685–1692. https://doi.org/10.1080/15384101.2016.1172158.

Demarco, R.S., Struckhoff, E.C., Lundquist, E.A., 2012. The Rac GTP exchange factor TIAM-1 acts with CDC-42 and the guidance receptor UNC-40/DCC in neuronal protrusion and axon guidance. PLoS Genet. 8, e1002665 https://doi.org/10.1371/journal.pgen.1002665.

Díaz-Balzac, C.A., Rahman, M., Lazaro-Pena, M.I., Martin Hernandez, L.A., Salzberg, Y., Aguirre-Chen, C., Kaprielian, Z., Bülow, H.E., 2016. Muscle- and skin-derived cues jointly orchestrate patterning of somatosensory dendrites. Curr. Biol. 26, 2379–2387. https://doi.org/10.1016/j.cub.2016.07.008.

Dong, X., Chiu, H., Park, Y.J., Zou, W., Zou, Y., Özkan, E., Chang, C., Shen, K., 2016. Precise regulation of the guidance receptor DMA-1 by KPC-1/Furin instructs dendritic branching decisions. eLife 5, 308. https://doi.org/10.7554/eLife.11008.

Dong, X., Liu, O.W., Howell, A.S., Shen, K., 2013. An extracellular adhesion molecule complex patterns dendritic branching and morphogenesis. Cell 155, 296–307. https://doi.org/10.1016/j.cell.2013.08.059.

Dong, X., Shen, K., Bulow, H.E., 2015. Intrinsic and extrinsic mechanisms of dendritic morphogenesis. Annu. Rev. Physiol. 77, 271–300. https://doi.org/10.1146/annurev-physiol-021014-071746.

Fuerst, P.G., Bruce, F., Tian, M., Wei, W., Elstrott, J., Feller, M.B., Erskine, L., Singer, J.H., Burgess, R.W., 2009. DSCAM and DSCAML1 function in self-avoidance in multiple cell types in the developing mouse retina. Neuron 64, 484–497. https://doi.org/10.1016/j.neuron.2009.09.027.

Gallo, G., 2006. RhoA-kinase coordinates F-actin organization and myosin II activity during semaphorin-3A-induced axon retraction. J. Cell Sci. 119, 3413–3423. https://doi.org/10.1242/jcs.03084.

Ghosh-Roy, A., Wu, Z., Goncharov, A., Jin, Y., Chisholm, A.D., 2010. Calcium and cyclic AMP promote axonal regeneration in Caenorhabditis elegans and require DLK-1 kinase. J. Neurosci. 30, 3175–3183. https://doi.org/10.1523/JNEUROSCI.5464-09.2010.

Gibson, D.A., Tymanskyj, S., Yuan, R.C., Leung, H.C., Lefebvre, J.L., Sanes, J.R., Chédotal, A., Le Ma, 2014. Dendrite self-avoidance requires cell-autonomous slit/robo signaling in cerebellar Purkinje cells. Neuron 81, 1040–1056. https://doi.org/10.1016/j.neuron.2014.01.009.

Grueber, W.B., Jan, L.Y., Jan, Y.N., 2003. Different levels of the homeodomain protein cut regulate distinct dendrite branching patterns of Drosophila multidendritic neurons. Cell 112, 805–818.

Grueber, W.B., Sagasti, A., 2010. Self-avoidance and tiling: mechanisms of dendrite and axon spacing. Cold Spring Harb. Perspect. Biol. 2 https://doi.org/10.1101/cshperspect.a001750 a001750–a001750.

Halevi, S., McKay, J., Palfreyman, M., Yassin, L., Eshel, M., Jorgensen, E., Treinin, M., 2002. The C. elegans ric-3 gene is required for maturation of nicotinic acetylcholine receptors. EMBO J. 21, 1012–1020. https://doi.org/10.1093/emboj/21.5.1012.

Hall, D.H., Treinin, M., 2011. How does morphology relate to function in sensory arbors? Trends Neurosci. 34, 443–451. https://doi.org/10.1016/j.tins.2011.07.004.

Hao, J.C., Yu, T.W., Fujisawa, K., Culotti, J.G., Gengyo-Ando, K., Mitani, S., Moulder, G., Barstead, R., Tessier-Lavigne, M., Bargmann, C.I., 2001. C. elegans slit acts in

midline, dorsal-ventral, and anterior-posterior guidance via the SAX-3/Robo receptor. Neuron 32, 25–38.
Harterink, M., Edwards, S.L., de Haan, B., Yau, K.W., van den Heuvel, S., Kapitein, L.C., Miller, K.G., Hoogenraad, C.C., 2018. Local microtubule organization promotes cargo transport in C. elegans dendrites. J. Cell Sci. 131, jcs223107. https://doi.org/10.1242/jcs.223107.
Hiramoto, M., Hiromi, Y., Giniger, E., Hotta, Y., 2000. The Drosophila Netrin receptor Frazzled guides axons by controlling Netrin distribution. Nature 406, 886–889. https://doi.org/10.1038/35022571.
Husson, S.J., Costa, W.S., Wabnig, S., Stirman, J.N., Watson, J.D., Spencer, W.C., Akerboom, J., Looger, L.L., Treinin, M., Miller Iii, D.M., Lu, H., Gottschalk, A., 2012. Optogenetic analysis of a nociceptor neuron and network reveals ion channels acting downstream of primary sensors. Curr. Biol. 22, 743–752. https://doi.org/10.1016/j.cub.2012.02.066.
Jan, Y.N., Jan, L.Y., 2010. Branching out: mechanisms of dendritic arborization. Nat. Rev. Neurosci. 11, 316–328. https://doi.org/10.1038/nrn2836.
Kim, M.D., Jan, L.Y., Jan, Y.N., 2006. The bHLH-PAS protein Spineless is necessary for the diversification of dendrite morphology of Drosophila dendritic arborization neurons. Genes Dev. 20, 2806–2819. https://doi.org/10.1101/gad.1459706.
Kramer, A.P., Stent, G.S., 1985. Developmental arborization of sensory neurons in the leech Haementeria ghilianii. II. Experimentally induced variations in the branching pattern. J. Neurosci. 5, 768–775.
Kravtsov, V., Oren-Suissa, M., Podbilewicz, B., 2017. The fusogen AFF-1 can rejuvenate the regenerative potential of adult dendritic trees by self-fusion. Development 144, 2364–2374. https://doi.org/10.1242/dev.150037.
Lefebvre, J.L., Kostadinov, D., Chen, W.V., Maniatis, T., Sanes, J.R., 2012. Protocadherins mediate dendritic self-avoidance in the mammalian nervous system. Nature 488, 517–521. https://doi.org/10.1038/nature11305.
Li, W., Kang, L., Piggott, B.J., Feng, Z., Xu, X.Z.S., 2011. The neural circuits and sensory channels mediating harsh touch sensation in Caenorhabditis elegans. Nat. Commun. 2, 315–319. https://doi.org/10.1038/ncomms1308.
Liang, X., Dong, X., Moerman, D.G., Shen, K., Wang, X., 2015. Sarcomeres pattern proprioceptive sensory dendritic endings through UNC-52/Perlecan in C. elegans. Dev. Cell 33, 388–400. https://doi.org/10.1016/j.devcel.2015.03.010.
Liao, C.-P., Li, H., Lee, H.-H., Chien, C.-T., Pan, C.-L., 2018. Cell-autonomous regulation of dendrite self-avoidance by the Wnt secretory factor MIG-14/Wntless. Neuron 98, 320–334. https://doi.org/10.1016/j.neuron.2018.03.031 e6.
Liu, O.W., Shen, K., 2011. The transmembrane LRR protein DMA-1 promotes dendrite branching and growth in C. elegans. Nat. Neurosci. https://doi.org/10.1038/nn.2978.
Liu, X., Wang, X., Shen, K., 2016. Receptor tyrosine phosphatase CLR-1acts in skin cells to promote sensory dendrite outgrowth. Dev. Biol. 413, 60–69. https://doi.org/10.1016/j.ydbio.2016.03.001.
Liu, X., Guo, X., Niu, L., Li, X., Sun, F., Hu, J., Wang, X., Shen, K., 2019. Atlastin-1 regulates morphology and function of endoplasmic reticulum in dendrites. Nat. Commun. 10, 568. https://doi.org/10.1038/s41467-019-08478-6.
Luo, L., 2002. Actin cytoskeleton regulation in neuronal morphogenesis and structural plasticity. Annu. Rev. Cell Dev. Biol. 18, 601–635. https://doi.org/10.1146/annurev.cellbio.18.031802.150501.
Maniar, T.A., Kaplan, M., Wang, G.J., Shen, K., Wei, L., Shaw, J.E., Koushika, S.P., Bargmann, C.I., 2011. UNC-33 (CRMP) and ankyrin organize microtubules and localize kinesin to polarize axon-dendrite sorting. Nat. Neurosci. 15, 48–56. https://doi.org/10.1038/nn.2970.
Matsuoka, R.L., Jiang, Z., Samuels, I.S., Nguyen-Ba-Charvet, K.T., Sun, L.O., Peachey, N.S., Chédotal, A., Yau, K.-W., Kolodkin, A.L., 2012. Guidance-cue control of horizontal cell morphology, lamination, and synapse formation in the mammalian outer retina. J. Neurosci. 32, 6859–6868. https://doi.org/10.1523/JNEUROSCI.0267-12.2012.
Matthews, B.J., Kim, M.E., Flanagan, J.J., Hattori, D., Clemens, J.C., Zipursky, S.L., Grueber, W.B., 2007. Dendrite self-avoidance is controlled by Dscam. Cell 129, 593–604. https://doi.org/10.1016/j.cell.2007.04.013.
Maurel, M., Chevet, E., Tavernier, J., Gerlo, S., 2014. Getting RIDD of RNA: IRE1 in cell fate regulation. Trends Biochem. Sci. 39, 245–254. https://doi.org/10.1016/j.tibs.2014.02.008.
McConnell, R.E., Edward van Veen, J., Vidaki, M., Kwiatkowski, A.V., Meyer, A.S., Gertler, F.B., 2016. A requirement for filopodia extension toward Slit during Robo-mediated axon repulsion. J. Cell Biol. 213, 261–274. https://doi.org/10.1083/jcb.201509062.
Mitchison, T.J., Cramer, L.P., 1996. Actin-based cell motility and cell locomotion. Cell 84, 371–379.
Moerman, D.G., Williams, B.D., 2006. Sarcomere assembly in C. elegans muscle. WormBook Online Rev. C Elegans Biol. 1–16. https://doi.org/10.1895/wormbook.1.81.1.
Mohammadi, A., Rodgers, J.B., Kotera, I., Ryu, W.S., 2013. Behavioral response of Caenorhabditis elegans to localized thermal stimuli. BMC Neurosci. 14 https://doi.org/10.1186/1471-2202-14-66, 1–1.
Mohler, W.A., Shemer, G., del Campo, J.J., Valansi, C., Opoku-Serebuoh, E., Scranton, V., Assaf, N., White, J.G., Podbilewicz, B., 2002. The type I membrane protein EFF-1 is essential for developmental cell fusion. Dev. Cell 2, 355–362.
Murray, A., Naeem, A., Barnes, S.H., Drescher, U., Guthrie, S., 2010. Slit and Netrin-1 guide cranial motor axon pathfinding via Rho-kinase, myosin light chain kinase and myosin II. Neural Dev. 5, 16. https://doi.org/10.1186/1749-8104-5-16.
Nath, R.D., Chow, E.S., Wang, H., Schwarz, E.M., Sternberg, P.W., 2016. C. elegans stress-induced sleep emerges from the collective action of multiple neuropeptides. Curr. Biol. 26, 2446–2455. https://doi.org/10.1016/j.cub.2016.07.048.
Nithianandam, V., Chien, C.-T., 2018. Actin blobs prefigure dendrite branching sites. J. Cell Biol. 217, 3731–3746. https://doi.org/10.1083/jcb.201711136.
Norris, A.D., Sundararajan, L., Morgan, D.E., Roberts, Z.J., Lundquist, E.A., 2014. The UNC-6/Netrin receptors UNC-40/DCC and UNC-5 inhibit growth cone filopodial protrusion via UNC-73/Trio, Rac-like GTPases and UNC-33/CRMP. Development 141, 4395–4405. https://doi.org/10.1242/dev.110437.
Ohtomi, M., 2010. Regulation of neurite extension by expression of LECT2 and neurotrophins based on findings in LECT2-knockout mice. Brain Res. 1311, 1–11. https://doi.org/10.1016/j.brainres.2009.11.010.
Ono, K., Ono, S., 2016. Two distinct myosin II populations coordinate ovulatory contraction of the myoepithelial sheath in the Caenorhabditis elegans somatic gonad. Mol. Biol. Cell 27, 1131–1142. https://doi.org/10.1091/mbc.E15-09-0648.
Oren-Suissa, M., Gattegno, T., Kravtsov, V., Podbilewicz, B., 2017. Extrinsic repair of injured dendrites as a paradigm for regeneration by fusion in Caenorhabditis elegans. Genetics 206, 215–230. https://doi.org/10.1534/genetics.116.196386.
Oren-Suissa, M., Hall, D.H., Treinin, M., Shemer, G., Podbilewicz, B., 2010. The fusogen EFF-1 controls sculpting of mechanosensory dendrites. Science 328, 1285–1288. https://doi.org/10.1126/science.1189095.
O'Brien, B., Miller III, D.M., Miller Iii, D.M., 2016. Neurodevelopment: three's a crowd, four is a receptor complex. Curr. Biol. 26, R799–R801. https://doi.org/10.1016/j.cub.2016.07.055.
O'Brien, B.M.J., Palumbos, S.D., Novakovic, M., Shang, X., Sundararajan, L., Miller III, D.M., 2017. Separate transcriptionally regulated pathways specify distinct classes of sister dendrites in a nociceptive neuron. Dev. Biol. 432, 248–257. https://doi.org/10.1016/j.ydbio.2017.10.009.
Pocock, R., Bénard, C.Y., Shapiro, L., Hobert, O., 2008. Functional dissection of the C. elegans cell adhesion molecule SAX-7, a homologue of human L1. Mol. Cell. Neurosci. 37, 56–68. https://doi.org/10.1016/j.mcn.2007.08.014.
Poirier, S., Mayer, G., 2013. The biology of PCSK9 from the endoplasmic reticulum to lysosomes: new and emerging therapeutics to control low-density lipoprotein cholesterol. Drug Des. Dev. Ther. 7, 1135–1148. https://doi.org/10.2147/DDDT.S36984.
Pollard, T.D., 2016. Actin and actin-binding proteins. Cold Spring Harb. Perspect. Biol. 8, a018226 https://doi.org/10.1101/cshperspect.a018226.
Port, F., Basler, K., 2010. Wnt trafficking: new insights into Wnt maturation, secretion and spreading. Traffic 11, 1265–1271. https://doi.org/10.1111/j.1600-0854.2010.01076.x.
Ramirez-Suarez, N.J., Belalcazar, H.M., Salazar, C.J., Beyaz, B., Raja, B., Nguyen, K.C.Q., Celestrin, K., Fredens, J., Færgeman, N.J., Hall, D.H., Bülow, H.E., 2019. Axon-dependent patterning and maintenance of somatosensory dendritic arbors. Dev. Cell 48, 229–244. https://doi.org/10.1016/j.devcel.2018.12.015 e4.
Richardson, C.E., Spilker, K.A., Cueva, J.G., Perrino, J., Goodman, M.B., Shen, K., 2014. PTRN-1, a microtubule minus end-binding CAMSAP homolog, promotes microtubule function in Caenorhabditis elegans neurons. eLife 3, e01498. https://doi.org/10.7554/eLife.01498.
Saito, A., Cai, L., Matsuhisa, K., Ohtake, Y., Kaneko, M., Kanemoto, S., Asada, R., Imaizumi, K., 2018. Neuronal activity-dependent local activation of dendritic unfolded protein response promotes expression of brain-derived neurotrophic factor in cell soma. J. Neurochem. 144, 35–49. https://doi.org/10.1111/jnc.14221.
Salzberg, Y., Coleman, A.J., Celestrin, K., Cohen-Berkman, M., Biederer, T., Henis-Korenblit, S., Bülow, H.E., 2017. Reduced insulin/insulin-like growth factor receptor signaling mitigates defective dendrite morphogenesis in mutants of the ER stress sensor IRE-1. PLoS Genet. 13, e1006579 https://doi.org/10.1371/journal.pgen.1006579.
Salzberg, Y., Díaz-Balzac, C.A., Ramirez-Suarez, N.J., Attreed, M., Tecle, E., Desbois, M., Kaprielian, Z., Bülow, H.E., 2013. Skin-derived cues control arborization of sensory dendritesin Caenorhabditis elegans. Cell 155, 308–320. https://doi.org/10.1016/j.cell.2013.08.058.
Salzberg, Y., Ramirez-Suarez, N.J., Bülow, H.E., 2014. The proprotein convertase KPC-1/Furin controls branching and self-avoidance of sensory dendrites in Caenorhabditis elegans. PLoS Genet. 10 https://doi.org/10.1371/journal.pgen.1004657 e1004657–13.
Schroeder, N.E., Androwski, R.J., Rashid, A., Lee, H., Lee, J., Barr, M.M., 2013. Dauer-specific dendrite arborization in C. elegans is regulated by KPC-1/Furin. Curr. Biol. 23, 1527–1535. https://doi.org/10.1016/j.cub.2013.06.058.
Slowik, V., Apte, U., 2017. Leukocyte cell-derived chemotaxin-2: it's role in pathophysiology and future in clinical medicine. Clin. Transl. Sci. 10, 249–259. https://doi.org/10.1111/cts.12469.
Smith, C.J., O'Brien, T., Treinin, M., Miller III, D.M., 2010. Time-lapse imaging and cell-specific expression profiling reveal dynamic branching and molecular determinants of a multi-dendritic nociceptor in C. elegans. Dev. Biol. 345, 18–33. https://doi.org/10.1016/j.ydbio.2010.05.502.
Smith, C.J., O'Brien, T., Chatzigeorgiou, M., Spencer, W.C., Feingold-Link, E., Husson, S.J., Hori, S., Mitani, S., Gottschalk, A., Schafer, W.R., Miller Iii, D.M., 2013. Sensory neuron fates are distinguishedby a transcriptional switchthat regulates dendrite branch stabilization. Neuron 79, 266–280. https://doi.org/10.1016/j.neuron.2013.05.009.
Smith, C.J., Watson, J.D., Vanhoven, M.K., Colón-Ramos, D.A., Miller III, D.M., 2012. Netrin (UNC-6) mediates dendritic self-avoidance. Nat. Neurosci. 15, 731–737. https://doi.org/10.1038/nn.3065.
Spencer, W.C., McWhirter, R., Miller, T., Strasbourger, P., Thompson, O., Hillier, L.W., Waterston, R.H., Miller III, D.M., 2014. Isolation of specific neurons from C. elegans larvae for gene expression profiling. PLoS One 9, e112102. https://doi.org/10.1371/journal.pone.0112102.
Sulston, J.E., Horvitz, H.R., 1977. Post-embryonic cell lineages of the nematode, Caenorhabditis elegans. Dev. Biol. 56, 110–156.

Sun, L., Shay, J., McLoed, M., Roodhouse, K., Chung, S.H., Clark, C.M., Pirri, J.K., Alkema, M.J., Gabel, C.V., 2014. Neuronal regeneration in C. elegans requires subcellular calcium release by ryanodine receptor channels and can be enhanced by optogenetic stimulation. J. Neurosci. 34, 15947–15956. https://doi.org/10.1523/JNEUROSCI.4238-13.2014.

Sundararajan, L., Smith, C., Watson, J., Millis, B., Tyska, M., Miller, D., 2018. Netrin/UNC-6 triggers actin assembly and non-muscle myosin activity to drive dendrite retraction in the self-avoidance response. bioRxiv 1–56. https://doi.org/10.1101/492769.

Takenawa, T., Suetsugu, S., 2007. The WASP-WAVE protein network: connecting the membrane to the cytoskeleton. Nat. Rev. Mol. Cell Biol. 8, 37–48. https://doi.org/10.1038/nrm2069.

Tang, L.T., Díaz-Balzac, C.A., Rahman, M., Ramirez-Suarez, N.J., Salzberg, Y., Lazaro-Pena, M.I., Bülow, H.E., 2019. TIAM-1/GEF can shape somatosensory dendrites independently of its GEF activity by regulating F-actin localization. eLife 8, 507. https://doi.org/10.7554/eLife.38949.

Taylor, C.A., Yan, J., Howell, A.S., Dong, X., Shen, K., 2015. RAB-10 regulates dendritic branching by balancing dendritic transport. PLoS Genet. 11, e1005695 https://doi.org/10.1371/journal.pgen.1005695.

Tsalik, E.L., Niacaris, T., Wenick, A.S., Pau, K., Avery, L., Hobert, O., 2003. LIM homeobox gene-dependent expression of biogenic amine receptors in restricted regions of the C. elegans nervous system. Dev. Biol. 263, 81–102.

Wadsworth, W.G., 2002. Moving around in a worm: netrin UNC-6 and circumferential axon guidance in C. elegans. Trends Neurosci. 25, 423–429.

Wadsworth, W.G., Bhatt, H., Hedgecock, E.M., 1996. Neuroglia and pioneer neurons express UNC-6 to provide global and local netrin cues for guiding migrations in C. elegans. Neuron 16, 35–46.

Watson, J.D., Wang, S., Stetina, Von, S.E., Spencer, W.C., Levy, S., Dexheimer, P.J., Kurn, N., Heath, J.D., Miller III, D.M., 2008. Complementary RNA amplification methods enhance microarray identification of transcripts expressed in the C. elegans nervous system. BMC Genom. 9, 84. https://doi.org/10.1186/1471-2164-9-84.

Way, J.C., Chalfie, M., 1989. The mec-3 gene of Caenorhabditis elegans requires its own product for maintained expression and is expressed in three neuronal cell types. Genes Dev. 3, 1823–1833.

Wei, X., Howell, A.S., Dong, X., Taylor, C.A., Cooper, R.C., Zhang, J., Zou, W., Sherwood, D.R., Shen, K., 2015. The unfolded protein response is required for dendrite morphogenesis. eLife 4, e06963. https://doi.org/10.7554/eLife.06963.

White, J.G., Southgate, E., Thomson, J.N., Brenner, S., 1986. The structure of the nervous system of the nematode Caenorhabditis elegans, 314, 1–340.

Yamagoe, S., Mizuno, S., 1996. Molecular cloning of human and bovine LECT2 having a neutrophil chemotactic activity and its specific expression in the liver. Biochim. Biophys. Acta Biomembr. 1396, 105–116.

Yan, J., Chao, D.L., Toba, S., Koyasako, K., Yasunaga, T., Hirotsune, S., Shen, K., 2013. Kinesin-1 regulates dendrite microtubule polarity in Caenorhabditis elegans, 2, e00133. https://doi.org/10.7554/eLife.00133.

Yassin, L., Samson, A.O., Halevi, S., Eshel, M., Treinin, M., 2002. Mutations in the extracellular domain and in the membrane-spanning domains interfere with nicotinic acetylcholine receptor maturation. Biochemistry 41, 12329–12335.

Yip, Z.C., Heiman, M.G., 2016. Duplication of a single neuron in C. elegans reveals a pathway for dendrite tiling by mutual repulsion. Cell Rep. 15, 2109–2117. https://doi.org/10.1016/j.celrep.2016.05.003.

Zhu, T., Liang, X., Wang, X.-M., Shen, K., 2017. Dynein and EFF-1 control dendrite morphology by regulating the localization pattern of SAX-7 in epidermal cells. J. Cell Sci. 130, 4063–4071. https://doi.org/10.1242/jcs.201699.

Zou, W., Dong, X., Broederdorf, T.R., Shen, A., Kramer, D.A., Shi, R., Liang, X., Miller III, D.M., Xiang, Y.K., Yasuda, R., Chen, B., Shen, K., 2018. A dendritic guidance receptor complex brings together distinct actin regulators to drive efficient F-actin assembly and branching. Dev. Cell 45, 362–375. https://doi.org/10.1016/j.devcel.2018.04.008 e3.

Zou, W., Shen, A., Dong, X., Tugizova, M., Xiang, Y.K., Shen, K., 2016. A multi-protein receptor-ligand complex underlies combinatorial dendrite guidance choices in C. elegans. eLife 5, e18345. https://doi.org/10.7554/eLife.18345.

Zou, W., Yadav, S., DeVault, L., Nung Jan, Y., Sherwood, D.R., 2015. RAB-10-Dependent membrane transport is required for dendrite arborization. PLoS Genet. 11, e1005484 https://doi.org/10.1371/journal.pgen.1005484.